JGR Atmospheres

RESEARCH ARTICLE
10.1029/2020JD033583

# Regional Characteristics of Atmospheric Sulfate Formation in East Antarctica Imprinted on $^{17}$O-Excess Signature

S. Ishino[1,2], S. Hattori[1], M. Legrand[3], Q. Chen[4], B. Alexander[4], J. Shao[4,5], J. Huang[4], L. Jaeglé[4], B. Jourdain[3], S. Preunkert[3], A. Yamada[6], N. Yoshida[1,7], and J. Savarino[3]

[1]Department of Chemical Science and Engineering, School of Materials and Chemical Technology, Tokyo Institute of Technology, Yokohama, Japan, [2]National Institute of Polar Research, Research Organization of Information and Systems, Tokyo, Japan, [3]Univ. Grenoble Alpes, CNRS, IRD, Grenoble INP, Institut des Géosciences de l'Environnement (IGE), Grenoble, France, [4]Department of Atmospheric Sciences, University of Washington, Seattle, WA, USA, [5]College of Flight Technology, Civil Aviation University of China, Tianjin, China, [6]Toshima Electric Ltd., Tokyo, Japan, [7]Earth-Life Science Institute, Tokyo Institute of Technology, Tokyo, Japan

**Key Points:**

- Regional characteristics of atmospheric sulfate formation were probed by $^{17}$O-excess ($\Delta^{17}$O) of sulfate at inland and coastal East Antarctica
- Specifically, high $\Delta^{17}$O in spring–summer at inland suggests that chemical destruction of methanesulfonate ($MS^-$) on the Antarctic Plateau produces sulfate
- Existing gap between $\Delta^{17}$O of sulfate in the atmosphere and ice can be reconciled by $MS^-$ destruction in snow

**Supporting Information:**

- Supporting Information S1
- Table S1
- Data Set S1
- Data Set S2
- Data Set S3

**Correspondence to:**
S. Hattori,
hattori.s.ab@m.titech.ac.jp;
shohato@gmail.com

**Citation:**
Ishino, S., Hattori, S., Legrand, M., Chen, Q., Alexander, B., Shao, J., et al. (2021). Regional characteristics of atmospheric sulfate formation in East Antarctica imprinted on $^{17}$O-excess signature. *Journal of Geophysical Research: Atmospheres*, *126*, e2020JD033583. https://doi.org/10.1029/2020JD033583

Received 14 AUG 2020
Accepted 13 FEB 2021

**Author Contributions:**
**Conceptualization:** S. Hattori, B. Alexander, J. Savarino
**Data curation:** S. Ishino, S. Hattori
**Formal analysis:** S. Ishino, S. Hattori, M. Legrand, Q. Chen, B. Alexander, J. Savarino



## Abstract

$^{17}$O-excess ($\Delta^{17}O = \delta^{17}O - 0.52 \times \delta^{18}O$) of sulfate trapped in Antarctic ice cores has been proposed as a potential tool for assessing past oxidant chemistry, while insufficient understanding of atmospheric sulfate formation around Antarctica hampers its interpretation. To probe influences of regional specific chemistry, we compared year-round observations of $\Delta^{17}$O of non-sea-salt sulfate in aerosols ($\Delta^{17}O(SO_4^{2-})_{nss}$) at Dome C and Dumont d'Urville, inland and coastal sites in East Antarctica, throughout the year 2011. Although $\Delta^{17}O(SO_4^{2-})_{nss}$ at both sites showed consistent seasonality with summer minima (~1.0‰) and winter maxima (~2.5‰) owing to sunlight-driven changes in the relative importance of $O_3$ oxidation to OH and $H_2O_2$ oxidation, significant intersite differences were observed in austral spring–summer and autumn. The cooccurrence of higher $\Delta^{17}O(SO_4^{2-})_{nss}$ at inland (2.0‰ ± 0.1‰) than the coastal site (1.2‰ ± 0.1‰) and chemical destruction of methanesulfonate ($MS^-$) in aerosols at inland during spring–summer (October–December), combined with the first estimated $\Delta^{17}O(MS^-)$ of ~16‰, implies that $MS^-$ destruction produces sulfate with high $\Delta^{17}O(SO_4^{2-})_{nss}$ of ~12‰. If contributing to the known postdepositional decrease of $MS^-$ in snow, this process should also cause a significant postdepositional increase in $\Delta^{17}O(SO_4^{2-})_{nss}$ over 1‰, that can reconcile the discrepancy between $\Delta^{17}O(SO_4^{2-})_{nss}$ in the atmosphere and ice. The higher $\Delta^{17}O(SO_4^{2-})_{nss}$ at the coastal site than inland during autumn (March–May) may be associated with oxidation process involving reactive bromine and/or sea-salt particles around the coastal region.

## Plain Language Summary

It has been proposed that the past variations of atmospheric oxidants (e.g., ozone) might be estimated using $^{17}$O-excess, a unique isotopic signature, of sulfate trapped in polar ice cores. However, chemical processes altering $^{17}$O-excess of sulfate in the atmosphere and also in snow after deposition have not been fully understood, limiting the practicality of the signature. We investigated regional differences in $^{17}$O-excess of sulfate in aerosol particles at inland and coastal sites in East Antarctica. Our results suggest that the chemical destruction of atmospheric methanesulfonate, the second abundant sulfur compound in Antarctic aerosols, produces sulfate with significantly high $^{17}$O-excess signature at inland Antarctica. If also occurring in snow, this process can explain the existing gap of the signature between the atmosphere and ice. These results should be taken into account through future studies investigating the past atmospheric compositions using this signature in ice cores.

## 1. Introduction

Sulfate is a major component of impurities trapped in Antarctic ice cores and widely used for reconstruction of paleoclimate conditions (e.g., Legrand & Mayewski, 1997). For instance, since the main source of sulfate in Antarctica is oxidation of dimethyl sulfide (DMS) emitted by marine biota (Cosme et al., 2005; Minikin et al., 1998), sulfate in the Antarctic ice cores are often discussed in light of the past bioproductivity of the Southern Ocean (Goto-Azuma et al., 2019; Legrand et al., 1988; Wolff et al., 2006). In addition to the use of sulfate content in ice cores, $^{17}$O-excess ($\Delta^{17}O = \delta^{17}O - 0.52 \times \delta^{18}O$) of sulfate ($\Delta^{17}O(SO_4^{2-})$) is expected

**Funding acquisition:** S. Hattori, B. Alexander, N. Yoshida, J. Savarino
**Investigation:** S. Ishino, S. Hattori, M. Legrand, Q. Chen, B. Alexander, B. Jourdain, S. Preunkert, J. Savarino
**Methodology:** S. Ishino, S. Hattori, J. Savarino
**Project Administration:** S. Hattori, B. Alexander, N. Yoshida
**Resources:** S. Hattori, N. Yoshida, J. Savarino
**Software:** S. Ishino, S. Hattori, Q. Chen, B. Alexander, J. Shao, J. Huang, L. Jaeglé, A. Yamada
**Supervision:** S. Hattori, B. Alexander, N. Yoshida, J. Savarino
**Validation:** S. Ishino, S. Hattori
**Writing – original draft:** S. Ishino, S. Hattori
**Writing – review & editing:** S. Ishino, S. Hattori, M. Legrand, Q. Chen, B. Alexander, J. Savarino

to be a potential tool assessing past oxidant chemistry involving ozone ($O_3$) and hydroxyl radicals (OH), those playing central roles in tropospheric chemistry but not directly preserved in ice cores (Alexander & Mickley, 2015; Kunasek et al., 2010; Murray et al., 2014; Sofen et al., 2014). $\Delta^{17}O(SO_4^{2-})$ is generally assumed to reflect relative importance of different sulfate formation pathways, since the sulfate produced via gas-phase oxidation of $SO_2$ by OH possesses $\Delta^{17}O = 0‰$ (Barkan & Luz, 2005; Dubey et al., 1997), whereas those produced via aqueous-phase oxidations of dissolved $SO_2$ ($S(IV) = SO_2{\cdot}H_2O + HSO_3^- + SO_3^{2-}$) by $O_3$ or hydrogen peroxide ($H_2O_2$) possess $\Delta^{17}O > 0‰$ (Savarino & Thiemens, 1999; Savarino et al., 2000; Vicars & Savarino, 2014). Sofen et al. (2014) observed a 1.1‰ increase of $\Delta^{17}O(SO_4^{2-})$ within the early nineteenth century in West Antarctic Ice Sheet Divide ice cores, probably suggesting an increase of $O_3$ oxidation relative to OH and $H_2O_2$ oxidation in sulfate formation in the mid-southern to high-southern latitude region. However, they estimated by their box model that a 1.1‰ increase of $\Delta^{17}O(SO_4^{2-})$ requires a 260% increase of relative abundance of $O_3$/OH, which they concluded was highly implausible given a 26% increase of $O_3$/OH from a chemistry transport model estimate for the Southern Hemisphere extratropics. Based on such results, they pointed out deficiencies in the understanding of sulfate formation other than the recognized $SO_2$ oxidation by OH, $H_2O_2$, and $O_3$. Furthermore, there is increasing evidence for a significant difference between the $\Delta^{17}O(SO_4^{2-})$ in aerosol samples (ca., 1.5‰; Hill-Falkenthal et al., 2013; Ishino et al., 2017; Walters et al., 2019) and those in ice cores corresponding to the present-day climate conditions (ca., 3‰; Alexander et al., 2002, 2003; Kunasek et al., 2010; Sofen et al., 2014). Despite the significance of this ~1.5‰ shift in $\Delta^{17}O(SO_4^{2-})$ compared to the observed variability in ice cores (1.3‰–4.8‰ for glacial–interglacial time scale), there has been no study pointing it out so far. Thus, the interpretation of ice core $\Delta^{17}O(SO_4^{2-})$ records requires a better understanding of atmospheric sulfate formation in Antarctica.

In Antarctica, where the impact of anthropogenic emissions is still insignificant, there exist unique oxidative conditions associated with natural emissions of reactive trace gases from snow and sea-ice surfaces (Grannas et al., 2007; Simpson et al., 2007). One characteristic is drastic enhancements of photochemical oxidants, represented by OH and $O_3$, over the Antarctic Plateau after polar sunrise to the austral midsummer (Crawford et al., 2001; Grannas et al., 2007; Mauldin et al., 2001), which is mainly triggered by nitrate photolysis within snowpack (Erbland et al., 2013; Frey et al., 2009; Noro et al., 2018) emitting reactive nitrogen species (e.g., $NO_x$) to the atmosphere (Davis et al., 2008). It has been recently found that the concentration of methanesulfonate ($MS^-$), a second abundant product of DMS oxidation after sulfate, suddenly decreased in the highly oxidative atmosphere in midsummer at Dome C, inland Antarctica (Legrand, Preunkert, Weller, et al., 2017). It was hypothesized that this may be due to a chemical destruction of $MS^-$, possibly into sulfate, but the hypothesis needs confirmation and quantification. Since it is also known that $MS^-$ is partially lost in snow after its deposition (Delmas et al., 2003; Wagnon et al., 1999; Weller et al., 2004), it is important to examine the impact of $MS^-$ destruction on sulfate formation and $\Delta^{17}O(SO_4^{2-})_{nss}$ values in snow and ice. Another characteristic is the elevated reactive bromine over coastal Antarctica during austral spring, as indicated from satellite observations of tropospheric BrO columns (Theys et al., 2011). Hypobromous acid (HOBr), which is produced from the $BrO + HO_2$ reaction, was proposed to represent up to 50% of total sulfate production in the summertime marine boundary layer (MBL) over the Southern Ocean (Chen et al., 2016). The contribution of this reaction is thus expected to be also significant in the Antarctic troposphere.

There are only a few reports of $\Delta^{17}O(SO_4^{2-})$ observations in the present Antarctic atmosphere, and little is known about the influence of characteristic oxidation processes in Antarctica on $\Delta^{17}O(SO_4^{2-})$. $\Delta^{17}O(SO_4^{2-})$ observations of aerosols at three different sites, Dome C (Hill-Falkenthal et al., 2013) and South Pole (Walters et al., 2019) on the Antarctic Plateau and coastal Antarctic station Dumont d'Urville (DDU) (Ishino et al., 2017), show similar seasonality with minima in the austral summer and higher values in the autumn to spring, which likely reflects a seasonal shift from OH- and $H_2O_2$- to $O_3$-dominated chemistry. In addition, Ishino et al. (2017) and Walters et al. (2019) suggested the possibility of an increased contribution of S(IV) + HOBr during austral spring at DDU and summer at South Pole, respectively, based on the relatively low $\Delta^{17}O(SO_4^{2-})$ in those seasons. However, the importance of S(IV) + HOBr remains inconclusive, since both results in those two previous works can also be explained by the contribution of OH and $H_2O_2$ oxidation. Meanwhile, there is no study investigating the possible impact of $MS^-$ destruction to $\Delta^{17}O(SO_4^{2-})$ so far. To evaluate the consequences of characteristic chemical processes to $\Delta^{17}O(SO_4^{2-})$ in Antarctica, a comparison of the isotope signatures at inland and coastal sites can be helpful, since the $MS^-$ destruction

appears most significant on the Antarctic Plateau (Legrand, Preunkert, Weller, et al., 2017) while reactive bromine is more abundant in coastal regions (Theys et al., 2011). Here, we conduct an intersite comparison of year-round $\Delta^{17}O(SO_4^{2-})$ values of atmospheric sulfate, using weekly $\Delta^{17}O(SO_4^{2-})$ observations newly obtained for the inland site Dome C in this study and those previously obtained for coastal site DDU (Ishino et al., 2017) in the same year 2011. We also compare the observations with the $\Delta^{17}O(SO_4^{2-})$ values estimated using a global chemical-transport model GEOS-Chem, which includes reactive bromine production from sea-salt aerosols that originate from both the open ocean and blowing snow sublimation over sea-ice (Huang et al., 2020).

## 2. Materials and Methods

### 2.1. Aerosol Sampling and Measurement of Soluble Species

Aerosol samples were collected at Dome C (75°10′S, 123°30′E; 3,233 m above sea level), located on the East Antarctic Plateau 1,100 km from the nearest coast. The aerosol sampling is performed continuously at Dome C from the year 2010 as a part of Sulfate and Nitrate Evolution at Dome C (SUNITEDC) program (e.g., Erbland et al., 2013). Bulk aerosol was collected on glass fiber filters using high-volume air sampler (HVAS; General Metal Works GL 2000H Hi Vol TSP; Tisch Environmental, Cleves, OH) at the flow rate of 1.7 $m^3$ $min^{-1}$ with time resolution of 1–2 weeks. The HVAS was placed at ∼1 km distant from the main building of research activity at Dome C. A field blank was checked once per month by mounting filters onto the filter holder and running for 1 min. After each collection run, filters were removed from the HVAS and wrapped in aluminum foil, which were sealed in plastic bags, stored at −20°C, and shipped to Institut des Géosciences de l'Environnement (Grenoble, France) for chemical analyses. Samples collected during January–December 2011 were used in this study.

The procedures for extraction and quantification of soluble species concentrations in aerosols are detailed in Ishino et al. (2019). Some anions ($NO_3^-$ and $SO_4^{2-}$) and cations ($K^+$, $Mg^{2+}$, and $Ca^{2+}$) were measured at Tokyo Tech using ion chromatograph ICS2100, DIONEX with a guard column (Dionex IonPac AG19) and a separation column (Dionex IonPac AS19) for anions, and 881 Compact IC Pro, Metrohm with a guard column (Metrosep C4 S-Guard/4.0) and a separation column (Metrosep C 4-150/4.0) for cations. Considering high blank loading on filters or the lack of ion standard materials at Tokyo Tech, the concentration of other ions ($MS^-$, $Cl^-$, $Br^-$, oxalate ($C_2O_4^{2-}$), and $Na^+$) were obtained from other aerosol samples as described in Legrand, Preunkert, Wolff, et al. (2017) and Legrand, Preunkert, Weller, et al. (2017). The measured ion concentrations were corrected for blank values and reported as atmospheric concentration in standard temperature and pressure ($T = 273.15$ K, $p = 101{,}325$ Pa) based on meteorological data of Dome C provided by IPEV/PNRA (www.climantartide.it). The uncertainties were estimated based on the typical uncertainty of the ion chromatography analysis (5%).

### 2.2. Oxygen Isotope Measurements of Sulfate ($\Delta^{17}O(SO_4^{2-})$)

$\Delta^{17}O(SO_4^{2-})$ values were measured at Tokyo Tech with an isotope ratio mass spectrometer (IRMS) (MAT253; Thermo Fisher Scientific, Bremen, Germany), coupled with an in-house measurement system built following original setup by Savarino et al. (2001) and a series of improvements (Geng et al., 2013; Schauer et al., 2012). The detailed method is described in Ishino et al. (2017). Briefly, 1 μmol of $SO_4^{2-}$ was separated from other anions using ion chromatography and chemically converted to silver sulfate ($Ag_2SO_4$) using ion exchange resin. $O_2$ produced via thermal decomposition of the $Ag_2SO_4$ at 1,000°C within a high temperature conversion elemental analyzer (TC/EA; Thermo Fisher Scientific) was analyzed for isotopic compositions with the IRMS system. The interlaboratory calibrated standards (Sulf-α, β, and ε; Schauer et al., 2012) were used to assess the accuracy of our measurements of our working standards. Measured $\Delta^{17}O(SO_4^{2-})$ was corrected for oxygen isotope exchange with quartz ($\Delta^{17}O = 0$‰; Matsuhisa et al., 1979) by estimating the magnitude of isotopic exchange based on the set of working standard measurements along with the sample measurement runs as described in Schauer et al. (2012). The precision (1$\sigma$) of corrected $\Delta^{17}O$ was ±0.2‰ based on replicate analyses ($n = 35$) of our working standard C ($\Delta^{17}O = 8.4$‰).

Since sea-salt sulfate aerosols (ss-$SO_4^{2-}$) are not impacted by atmospheric oxidation processes (i.e., $\Delta^{17}O(SO_4^{2-})_{ss} = 0‰$), both total sulfate concentrations and $\Delta^{17}O$ values were corrected for their ss-$SO_4^{2-}$ component to obtain their non-sea-salt sulfate (nss-$SO_4^{2-}$) content, using the following Equations 1 and 2:

$$\left[SO_4^{2-}\right]_{nss} = \left[SO_4^{2-}\right]_{total} - k \times \left[Na^+\right] \quad (1)$$

$$\Delta^{17}O\left(SO_4^{2-}\right)_{nss} = \frac{\left[SO_4^{2-}\right]_{total}}{\left[SO_4^{2-}\right]_{nss}} \times \Delta^{17}O\left(SO_4^{2-}\right)_{total} \quad (2)$$

where "total" is the sum of ss- and nss-$SO_4^{2-}$ components; $k$ is the mass ratio of $[SO_4^{2-}]_{ss}/[Na^+]$ in seawater (0.25; Holland et al., 1986). To take into account sea-salt chemical fractionation processes that occur in the Antarctic region in winter, when temperatures drop below −8°C in the presence of sea-ice (Wagenbach et al., 1998), $k$ value of 0.16 ± 0.05 (Legrand, Preunkert, Wolff, et al., 2017) was applied from May to October. Equation 2 represents the isotope mass balance equation between ss- and nss-$SO_4^{2-}$, with $\Delta^{17}O(SO_4^{2-})_{ss} = 0‰$. Note that the sea-salt fractionation is a chemical fractionation and should not shift $\Delta^{17}O$. The uncertainties of ion concentration measurement (±5%), $\Delta^{17}O$ measurement (±0.2‰), and the $k$ value were propagated to $\Delta^{17}O(SO_4^{2-})_{nss}$. The obtained uncertainty of $\Delta^{17}O(SO_4^{2-})_{nss}$ was ±0.3‰ on average, while reaches ±1.1‰ at maximum in the austral midwinter when the $[SO_4^{2-}]_{nss}/[SO_4^{2-}]_{total}$ is minimum.

### 2.3. Complementary Data

The $\Delta^{17}O(SO_4^{2-})_{nss}$ at Dome C were compared to those previously obtained at DDU (Ishino et al., 2017) in the same year 2011. The intersite difference was evaluated at weekly resolution by subtracting the $\Delta^{17}O(SO_4^{2-})_{nss}$ of each DDU sample from that of each Dome C sample collected in the closest time period, hereafter denoted $\Delta_{DC-DDU}$. Note that, at DDU, aerosol samples were collected separately for coarse (>1 μm) and fine (<1 μm) mode particles and the $\Delta^{17}O(SO_4^{2-})_{nss}$ was measured for fine mode (Ishino et al., 2017). The results were also compared to data sets of oxidants available year round at both Dome C and DDU, $O_3$ mixing ratios (Legrand, Preunkert, et al., 2016) and an estimate of total gaseous inorganic bromine ($[Br_y^*] = [HBr] + [HOBr] + 0.9[Br_2] + 0.4[BrO] + [BrNO_2] + [BrONO_2] + [Br]$) (Legrand, Yang, et al., 2016), as indicators of regional characteristic processes. Furthermore, $[MS^-]/[SO_4^{2-}]_{nss}$ mass ratios at Dome C (Legrand, Preunkert, Weller, et al., 2017) and DDU (Ishino et al., 2017) for the same year were used to examine the influence of chemical destruction of $MS^-$ on sulfate formation in the midsummer.

Additionally, to explore other possible processes influencing the $\Delta^{17}O(SO_4^{2-})_{nss}$ values, we investigated the relationship of $\Delta_{DC-DDU}$ to various chemical species observed at both sites. They include ion concentrations and acidity in aerosols ($[H^+]$), ratios of respective sulfur components, $[SO_4^{2-}]_{ss}/[SO_4^{2-}]_{total}$ ratio ($=1 - [SO_4^{2-}]_{nss}/[SO_4^{2-}]_{total}$, cf., Equation 1), and sulfur isotopic composition of non-sea-salt sulfate ($\delta^{34}S_{nss}$) (Ishino et al., 2019). $[H^+]$, estimated by using the following equation, was used to consider the contribution of aqueous-phase S(IV) + $O_3$ pathway, which is highly dependent on pH of liquid water in the atmosphere (Seinfeld & Pandis, 2006):

$$\begin{aligned}\left[H^+\right] = &\left(\left[Cl^-\right] + \left[Br^-\right] + \left[NO_3^-\right] + 2\left[SO_4^{2-}\right] + 2\left[C_2O_4^{2-}\right]\right) \\ &- \left(\left[Na^+\right] + \left[NH_4^+\right] + \left[K^+\right] + 2\left[Mg^{2+}\right] + 2\left[Ca^{2+}\right]\right)\end{aligned} \quad (3)$$

Also $[SO_4^{2-}]_{ss}/[SO_4^{2-}]_{total}$ was used to consider the potential importance of aqueous-phase S(IV) + $O_3$ reaction, since it has been recognized that S(IV) + $O_3$ proceeds rapidly in alkaline (pH ∼ 8) deliquescent solution in fresh sea-salt particles, subsequently shutting off due to acidification of sea-salt aerosol by the produced sulfate as well as by uptake of acidic gases such as $SO_2$, $HNO_3$, and $H_2SO_4$ (Alexander et al., 2005). $\delta^{34}S_{nss}$ was used to test the impact of sulfur sources on $\Delta^{17}O(SO_4^{2-})_{nss}$, since it reflects the relative contributions of marine biogenic (i.e., DMS-sourced) sulfate and nonmarine sulfate (nmb-$SO_4^{2-}$) including volcanic and continental sulfur sources (Ishino et al., 2019; Patris et al., 2000; Pruett et al., 2004). Additionally, $^{210}Pb$ was used to trace the contribution of long-range transport of continental submicron aerosols

(Elsasser et al., 2011; Legrand, Preunkert, Weller, et al., 2017). The relationships were examined separately for each season: December–January–February (DJF), March–April–May (MAM), June–July–August (JJA), September–October–November (SON), as well as October 29 to December 23 (OND), where the last one was defined based on the specifically positive $\Delta_{DC-DDU}$ values as explained later in Section 3.1. The obtained correlation coefficients ($r$ and $p$ values) are summarized in Table S1.

### 2.4. Model Description and Limitations

We used v11-02d of the GEOS-Chem global chemical-transport model of coupled aerosol–oxidant chemistry (Park et al., 2004; http://www.geos-chem.org/) to estimate the relative importance of sulfate formation processes and $\Delta^{17}O(SO_4^{2-})_{nss}$ in Antarctica. The model was run at 4° × 5° (latitude × longitude) horizontal resolution and 47 vertical levels up to 0.01 hPa, using the MERRA-2 assimilated meteorological data developed by the Global Modeling and Assimilation Office (GMAO) at NASA Goddard Space Flight Center. Simulations were performed for January–December 2011 after spinning up the model for 6 months prior to January 2011.

GEOS-Chem v11-02d includes detailed bromine chemistry as described in Parrella et al. (2012), Schmidt et al. (2016), Sherwen, Evans, et al. (2016), Sherwen, Schmidt, et al. (2016), and Chen et al. (2017). We also applied the reactive bromine emission scheme from sea-salt aerosols produced by blowing snow sublimation over sea-ice as described in Huang et al. (2018, 2020), with surface snow salinity of 0.1 and 0.03 psu over the Arctic and the Antarctic, respectively, for both first-year-ice and multi-year-ice. We assumed an enrichment factor of 9 for $Br^-/Na^+$ ratio in surface snow on sea-ice relative to seawater. Sea-salt emission from open ocean is simulated as a function of sea surface temperature and wind speed (Jaeglé et al., 2011), with updates from Huang and Jaeglé (2017) for cold ocean waters (SST < 5°C). The model is able to reproduce observed $Br_y$* concentrations at DDU from winter to spring (June–November), within the range of standard deviations of the monthly mean observations (Legrand, Yang, et al., 2016; Figure S1). DMS emission is parameterized as a function of sea surface temperature, wind speed, and DMS concentration in seawater obtained from Lana et al. (2011). Note that the model does not include reactive nitrogen emissions from snow nitrate photolysis (Grannas et al., 2007). This would lead to underestimates in oxidants over large area of the Antarctic continents, as exhibited by the underestimates in surface $O_3$ concentrations at both Dome C and DDU by a factor of ~1.5 (Figure 1e). Zatko et al. (2016) previously simulated that the inclusion of their snow $NO_x$ emission scheme in GEOS-Chem model will increase surface $O_3$ concentrations over the Antarctic continent by factors of 1.1–1.8. It is also recently pointed out that the underestimates in $O_3$ over the Southern Ocean are improved by the inclusion of a new $O_3$ deposition scheme associated with chemical reaction of $O_3$ with iodide on the ocean surface (Pound et al., 2020), which is not implemented in this study. Thus, the model has limitations in reproducing oxidants abundances, even though the general seasonality in $O_3$ with increases in winter and decreases in summer was reproduced (Figure 1e). We therefore note that our estimates in the relative contributions of sulfate formation processes bear an uncertainty associated with oxidant abundances despite good reproducibilities in $\Delta^{17}O(SO_4^{2-})_{nss}$ as shown later in Section 3.2 (Figure 2). The further precise prediction of $\Delta^{17}O(SO_4^{2-})_{nss}$ will require improvements in oxidants reproducibility in the future.

This version of the model includes gas-phase oxidation of $SO_2$ by OH, in-cloud aqueous-phase oxidations of S(IV) by $H_2O_2$, $O_3$ (Park et al., 2004), and HOBr (Chen et al., 2017), and oxidation of S(IV) by $O_3$ on sea-salt particles (Alexander et al., 2005). For in-cloud reactions, the cloud fraction and the liquid water content of cloud are obtained from MERRA-2 meteorological fields. For pH-dependent reactions such as in-cloud S(IV) + $O_3$ and S(IV) + HOBr, the effect of heterogeneity of cloud pH on S(IV) partitioning is accounted as described in Alexander et al. (2012). The model assumes in-cloud sulfate formations are prohibited at temperature <−15°C as originally designed by Park et al. (2004). We confirmed that this assumption limits the annual tropospheric sulfate production via aqueous-phase reactions to 13.8 Gg-S on the Antarctic Plateau (>68°S) in contrast to 137.0 Gg-S on the Southern Ocean (60°–68°S) within longitudes of 0°–180°E (Figure S3). This result is consistent with the limited occurrence frequency of super-cooled-liquid-water containing cloud (0%–10%) over the Antarctic Plateau compared to over the Southern Ocean (20%–60%) (Listowski et al., 2019). S(IV) + $O_3$ in sea salt is assumed as a function of $SO_2$ transfer rate constant from the gas to the aerosol phase, because the rate limiting step is not the aqueous-phase reaction rate of S(IV) + $O_3$

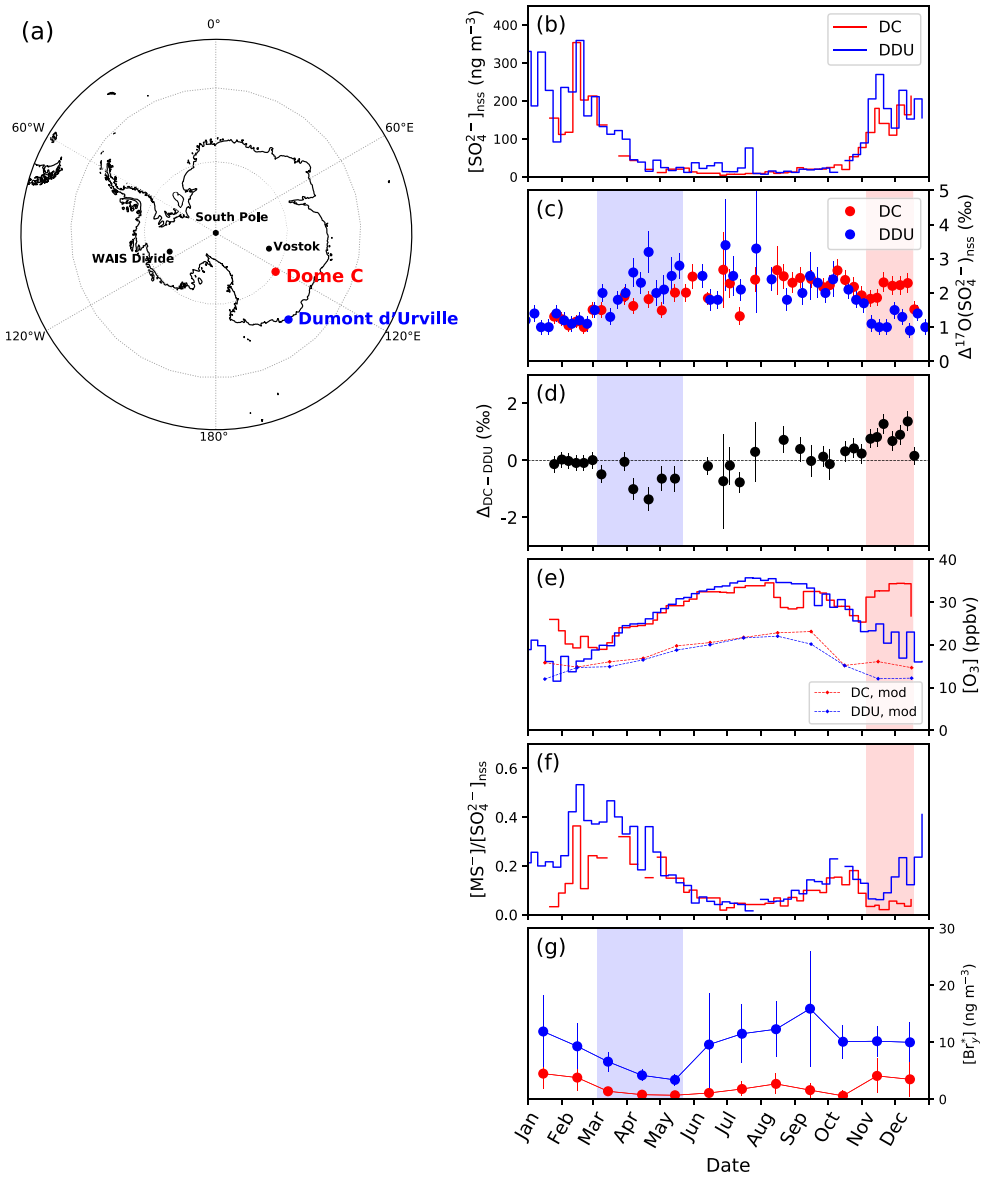


**Figure 1.** (a) Map of stations cited in this study. (b–g) Observed seasonal variations of (b) non-sea-salt sulfate concentrations, (c) $\Delta^{17}O(SO_4^{2-})_{nss}$ values (from this study and Ishino et al., 2017), (d) residual $\Delta^{17}O(SO_4^{2-})_{nss}$ values between Dome C and DDU ($\Delta_{DC-DDU}$, see Section 3.1), (e) ozone mixing ratios (Legrand, Preunkert, et al., 2016), (f) $[MS^-]/[SO_4^{2-}]_{nss}$ ratios (Ishino et al., 2017; Legrand, Preunkert, Weller, et al., 2017), and (g) total gaseous reactive bromine species ($Br_y$*) (Legrand, Yang, et al., 2016) at Dome C (red) and DDU (blue). Error bars in (b) and (c) represent the uncertainties propagated from analytical errors of $\Delta^{17}O(SO_4^{2-})_{nss}$ and concentration, and the uncertainty in $k$ value ($[SO_4^{2-}]_{ss}/[Na^+]$ mass ratio) in sea salt. The modeled ozone mixing ratios are also shown in (d). The red and blue shaded areas indicate the time periods showing positive and negative $\Delta_{DC-DDU}$ values, respectively. DDU, Dumont d'Urville.

in alkaline solution on fresh sea salt but is gas-phase diffusion of $SO_2$ to the aerosol surface (Alexander et al., 2005). This reaction is calculated only within MBL column, where the newly emitted sea salt is available, assuming that sea-salt alkalinity is rapidly consumed by this reaction in addition to the uptake of gas form $H_2SO_4$ and $HNO_3$ (Alexander et al., 2005).

We modified the model to tag sulfate produced via each oxidation pathway as different tracers which are transported, as originally described in Alexander et al. (2005). As atmospheric $SO_2$ rapidly attains isotopic equilibrium with $H_2O$ ($\Delta^{17}O$ = 0‰) (Barkan & Luz, 2005; Holt et al., 1981), $\Delta^{17}O$ value of sulfate produced

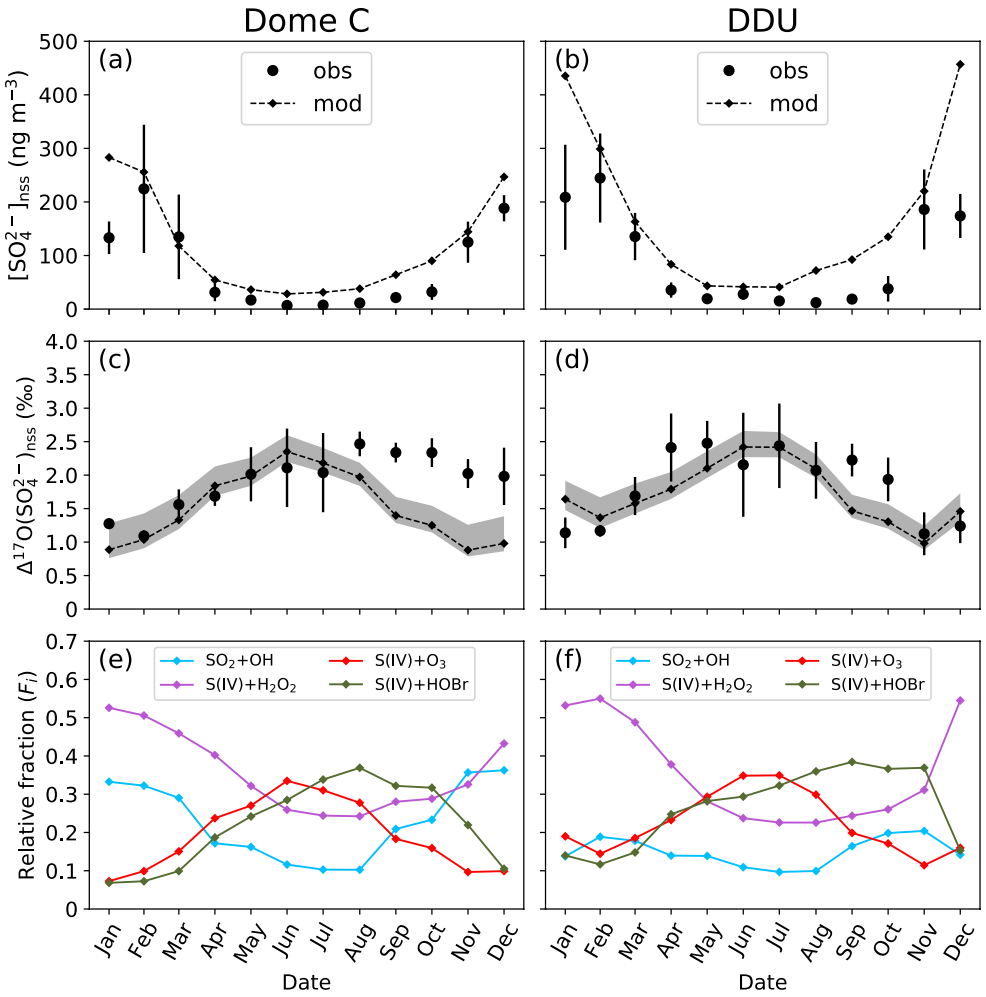


**Figure 2.** Comparison of observed and modeled values of (a, b) non-sea-salt sulfate concentration and (c, d) $\Delta^{17}O(SO_4^{2-})_{nss}$, and (e, f) calculated relative fraction of sulfate produced via different formation pathways ($F_i$, see Section 2.4), in the model. Left and right columns show results for Dome C and DDU, respectively. DDU, Dumont d'Urville.

via each formation pathway is determined by $\Delta^{17}O$ value of corresponding oxidant and their transferring factors (Savarino et al., 2000). Since OH also efficiently exchanges its oxygen isotopes with water vapor (Dubey et al., 1997), $\Delta^{17}O(OH)$ is also 0‰ under regions where water vapor is abundant (e.g., throughout most of the troposphere) (Lyons, 2001; Morin et al., 2007). Therefore, gas-phase $SO_2$ + OH produces sulfate with $\Delta^{17}O(SO_4^{2-})$ is assumed to be 0‰. Note that it has been previously suggested that $\Delta^{17}O(OH)$ can be 1‰–3‰ at Dome C (Savarino et al., 2016) due to the limited availability of water vapor in inland Antarctica. We also conducted the calculation with $\Delta^{17}O(OH)$ = 3‰ as a maximum case, which is expected to produce sulfate with $\Delta^{17}O(SO_4^{2-})$ = 0.75‰ with assuming oxygen atom transferring factor of 0.25. We note that there remains possibility that $\Delta^{17}O(OH)$ is higher than 3‰ (Savarino et al., 2016), that might cause underestimates in $\Delta^{17}O(SO_4^{2-})_{nss}$. The $\Delta^{17}O(SO_4^{2-})$ value of sulfate produced via aqueous-phase S(IV) + $H_2O_2$ is assumed to be 0.8‰ ± 0.2‰ based on $\Delta^{17}O(H_2O_2)$ of 1.6‰ ± 0.3‰ (Savarino & Thiemens, 1999) with a transferring factor of 0.5 (Savarino et al., 2000). Note that the $\Delta^{17}O(H_2O_2)$ is derived from only one set of observations at La Jolla, CA, and thus needs further verification in various environment in the future. For $\Delta^{17}O(O_3)$, among the whole sets of observations to the present, the two early studies using cryogenic technique had shown large variabilities (24.7‰ ± 11.4‰ and 26.5‰ ± 5.0‰; Johnston & Thiemens, 1997; Krankowsky et al., 1995). Such variabilities were much greater than those expected from the experimentally determined pressure and temperature dependency of $\Delta^{17}O(O_3)$, for example, a decrease of only ~2‰ for an pressure increase from 500 to 760 Torr (Morton et al., 1990; Thiemens & Jackson, 1990) and an increase of

only ~5‰ for an temperature increase from 260 to 320 K (Janssen et al., 2003; Morton et al., 1990). Based on these experimental data, it has been pointed out that these observations would have random errors associated with sampling artifacts (Mauersberger et al., 2003). Therefore, we exclude the data of these two studies from the consideration. Given the consistency of the $\Delta^{17}O(O_3)$ observations using nitrite-coated method among various locations and seasons including at Dome C and DDU (Ishino et al., 2017; Savarino et al., 2016; Vicars & Savarino, 2014), we decided to use the average value of the $\Delta^{17}O(O_3)$ observations, which comes to 25.6‰ ± 1.3‰. The $\Delta^{17}O(SO_4^{2-})$ for S(IV) + $O_3$, both in cloud and in sea salt, is assumed to be 6.4‰ ± 0.3‰, by a transferring factor of 0.25 (Savarino et al., 2000). Since aqueous-phase S(IV) oxidation by HOBr gives an oxygen atom from liquid water to produce sulfate (Fogelman et al., 1989; Liu et al., 2001; Troy & Margerum, 1991), the obtained $\Delta^{17}O(SO_4^{2-})$ is expected to be 0‰. Therefore, the $\Delta^{17}O(SO_4^{2-})_{nss}$ values in the model were calculated by adding all sulfate isotope tracers following the mass balance equation:

$$\Delta^{17}O\left(SO_4^{2-}\right)_{nss} = 0\cdot F_{SO_2+OH} + 0.8\cdot F_{S(IV)+H_2O_2} + 6.4\cdot F_{S(IV)+O_3} + 0\cdot F_{S(IV)+HOBr}, \quad (4)$$

$$F_i = \frac{\left[SO_4^{2-}\right]_i}{\left[SO_4^{2-}\right]_{SO_2+OH} + \left[SO_4^{2-}\right]_{S(IV)+H_2O_2} + \left[SO_4^{2-}\right]_{S(IV)+O_3} + \left[SO_4^{2-}\right]_{S(IV)+HOBr}}, \quad (5)$$

where $F_i$ represents the relative fraction of sulfate produced via each formation pathway $i$, respective to total sulfate concentration in each model grid. To calculate the $\Delta^{17}O(SO_4^{2-})_{nss}$ values and compare to the observations, the modeled $\Delta^{17}O(SO_4^{2-})_{nss}$ values of each grid including Dome C and DDU were mass-weighted averaged within the planetary boundary layer.

## 3. Results

### 3.1. $\Delta^{17}O(SO_4^{2-})_{nss}$ Values Observed at Dome C and Comparison to DDU

Figure 1 shows nss-$SO_4^{2-}$ concentrations ($[SO_4^{2-}]_{nss}$) and $\Delta^{17}O(SO_4^{2-})_{nss}$ at Dome C throughout 2011 in comparison to those previously reported for DDU (Ishino et al., 2017). Note that the concentration data are presented in Ishino et al. (2019). It is well established that $[SO_4^{2-}]_{nss}$ is enhanced during austral summer and reduced during winter, a seasonality that is driven by marine biogenic emission of DMS (Legrand, Preunkert, Weller, et al., 2017; Preunkert et al., 2007, 2008). This seasonal cycle in $[SO_4^{2-}]_{nss}$ is partially intensified by atmospheric dynamics due to enhanced efficiency of meridional long-range transport and the weakened inversion layer on the Antarctic Plateau during summer, as previously suggested by the similar seasonal cycle with $^{210}Pb$ (Elsässer et al., 2011; Legrand, Preunkert, Weller, et al., 2017). $\Delta^{17}O(SO_4^{2-})_{nss}$ show lower values in austral summer and higher values in winter, with monthly mean values ranging from 1.1‰ ± 0.1‰ in February to 2.5‰ ± 0.2‰ in August, with a mass-weighted annual average of 1.7‰ ± 0.1‰ (Table 1). These trends and values are generally consistent with previous observations at Dome C in 2010 (Hill-Falkenthal et al., 2013) as well as at DDU in 2011 (Ishino et al., 2017).

Figure 1d shows $\Delta_{DC-DDU}$, the differences in weekly $\Delta^{17}O(SO_4^{2-})_{nss}$ values between the two sites in the year 2011. Throughout most of the year, $\Delta_{DC-DDU}$ is 0‰ within the range of the estimated uncertainty. However, there are two specific time periods exhibiting $\Delta_{DC-DDU}$ values different from 0‰. One is from October to December, a transition from the austral spring to summer, when a group of positive $\Delta_{DC-DDU}$ values ranging 0.4‰ ± 0.3‰ to 1.4‰ ± 0.3‰ are observed. The second is found from March to May, the austral autumn, when negative $\Delta_{DC-DDU}$ values ranging −1.4‰ ± 0.6‰ to −0.5‰ ± 0.3‰ are observed. These $\Delta_{DC-DDU}$ values different from 0 suggest that sulfate at Dome C and DDU experienced different oxidation processes during their transport from source regions. The possible processes corresponding to these $\Delta_{DC-DDU}$ values are discussed in Section 4.

### 3.2. Modeled Sulfate Formation Processes and $\Delta^{17}O(SO_4^{2-})_{nss}$ Values

Figure 2 shows the modeled monthly $[SO_4^{2-}]_{nss}$ and mass-weighted $\Delta^{17}O(SO_4^{2-})_{nss}$ averaged within planetary boundary layer in the model grids including Dome C and DDU, with comparison to the monthly

**Table 1**
*Model Calculation of Relative Fraction of Sulfate Produced Via Different Formation Pathways and $\Delta^{17}O(SO_4^{2-})_{nss}$ Values in Each Season in Comparison to the Observed $\Delta^{17}O(SO_4^{2-})_{nss}$ Values (Seasonal Mean)*

| | | Observation | | Model | | | | |
|---|---|---|---|---|---|---|---|---|
| Site | Period | Number | $\Delta^{17}O(SO_4^{2-})_{nss}$ (‰) | $\Delta^{17}O(SO_4^{2-})_{nss}$ (‰)[a] | $F_{SO_2+OH}$ | $F_{S(IV)+H_2O_2}$ | $F_{S(IV)+O_3}$ | $F_{S(IV)+HOBr}$ |
| Dome C | Annual | 37 | 2.0 ± 0.5 (1.7 ± 0.1)[b] | 1.5 (1.4–1.8) | 0.23 | 0.34 | 0.18 | 0.25 |
| | DJF | 8 | 1.5 ± 0.5 | 1.0 (0.8–1.4) | 0.34 | 0.46 | 0.07 | 0.12 |
| | MAM | 9 | 1.8 ± 0.3 | 1.7 (1.6–2.0) | 0.21 | 0.38 | 0.21 | 0.20 |
| | JJA | 8 | 2.2 ± 0.5 | 2.2 (2.0–2.4) | 0.11 | 0.24 | 0.29 | 0.36 |
| | SON | 12 | 2.2 ± 0.2 | 1.2 (1.1–1.5) | 0.27 | 0.26 | 0.13 | 0.34 |
| | OND | 9 | 2.0 ± 0.3 | 1.0 (0.9–1.4) | 0.32 | 0.32 | 0.11 | 0.26 |
| DDU | Annual | 46 | 1.8 ± 0.7 (1.4 ± 0.1)[b] | 1.7 (1.6–2.0) | 0.15 | 0.34 | 0.21 | 0.29 |
| | DJF | 13 | 1.2 ± 0.2 | 1.5 (1.3–1.8) | 0.16 | 0.52 | 0.13 | 0.18 |
| | MAM | 12 | 2.2 ± 0.5 | 1.8 (1.7–2.1) | 0.15 | 0.37 | 0.23 | 0.24 |
| | JJA | 10 | 2.2 ± 0.8 | 2.3 (2.2–2.5) | 0.10 | 0.22 | 0.32 | 0.34 |
| | SON | 11 | 1.8 ± 0.6 | 1.3 (1.2–1.5) | 0.19 | 0.25 | 0.15 | 0.41 |
| | OND | 9 | 1.3 ± 0.3 | 1.3 (1.1–1.5) | 0.18 | 0.35 | 0.13 | 0.34 |

[a]Values shown in parentheses are possible ranges in case taking variabilities in $\Delta^{17}O$ of oxidants into account (see Section 2.4). [b]Mass-weighted average.

mean observations (±1$\sigma$). The modeled $[SO_4^{2-}]_{nss}$ reproduces the seasonality of the observations with austral summer maxima and winter minima, but the model overestimates $[SO_4^{2-}]_{nss}$ observations for summer (DJF) and winter (JJA) by a factor of 2 and 4 at Dome C, and 2 and 3 at DDU, respectively. Chen et al. (2018) reported that GEOS-Chem model run with DMS concentration in seawater from Lana et al. (2011) and without DMS oxidation by BrO, the condition used in this study, overestimates mixing ratio of DMS by a factor of 5 and 21 during summer and winter at DDU, respectively. This is likely a main reason for the overestimate of $[SO_4^{2-}]_{nss}$ at DDU and Dome C, as DMS oxidation is thought to be the main source of sulfate in these locations (e.g., Ishino et al., 2019; Minikin et al., 1998). We note that the overestimate of $[SO_4^{2-}]_{nss}$ could lead to an underestimate of $F_{S(IV)+O_3}$ and thus $\Delta^{17}O(SO_4^{2-})_{nss}$ in the model as we discuss in Section 4.

The model also reproduces the seasonality of $\Delta^{17}O(SO_4^{2-})_{nss}$ in the observations with austral summer minima and austral winter maxima, ranging from 0.9‰ (0.8‰–1.3‰, November and January) to 2.4‰ (2.2‰–2.6‰, June) and from 1.0‰ (0.9‰–1.2‰, November) to 2.4‰ (2.3‰–2.6‰, June–July) at Dome C and DDU, respectively. The modeled seasonality results from changes in the relative fractions of sulfate formed via different processes, $F_i$ in Equation 5 (Figures 2e and 2f; Table 1). During austral summer at Dome C, the relative fractions of sulfate formed by OH ($F_{SO_2+OH}$) and $H_2O_2$ ($F_{S(IV)+H_2O_2}$) increase to 34% and 49%, respectively (Table 1), because solar radiation induces production of these oxidants. In contrast, the $F_{S(IV)+O_3}$ increases to 31% during winter, when production of OH and $H_2O_2$ is diminished. Since S(IV) + $O_3$ is the only sulfate formation pathway that leads to $\Delta^{17}O(SO_4^{2-})_{nss} > 1$‰, the modeled $\Delta^{17}O(SO_4^{2-})_{nss}$ values (>2‰ in winter) mainly reflect the change in the relative importance of this pathway. The sulfate formed via S(IV) + HOBr ($F_{S(IV)+HOBr}$), which has $\Delta^{17}O(SO_4^{2-}) = 0$‰, also increases to 33% during winter, limiting the increase of $\Delta^{17}O(SO_4^{2-})_{nss}$ in the model. Although similar seasonal trends for sulfate formation pathways are found for DDU (Figure 2f), $F_{SO_2+OH}$ is significantly higher at Dome C (34% in summer) than DDU (16% in summer) (Table 1). This is because the model prohibits aqueous-phase sulfate production at temperatures lower than −15°C and therefore most sulfate formation along with the transport of precursors toward inland Antarctica occurs through gas-phase $SO_2$ + OH pathway.

As a result of these estimates in sulfate formation pathways, the model roughly reproduces the observed seasonality and magnitude of $\Delta^{17}O(SO_4^{2-})_{nss}$ (Figures 2c and 2d). However, the model largely underestimates observed $\Delta^{17}O(SO_4^{2-})_{nss}$ from August to December at Dome C by 0.5‰–1.1‰ (Figure 2c), partially

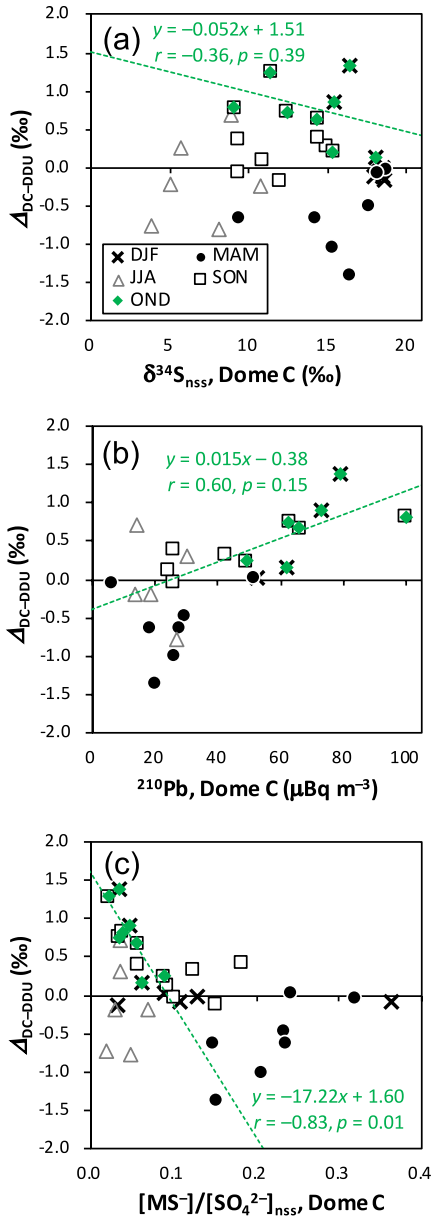


**Figure 3.** Variations of $\Delta_{DC-DDU}$ against (a) $\delta^{34}S_{nss}$, (b) $^{210}Pb$, and (c) $[MS^-]/[SO_4^{2-}]_{nss}$, at Dome C. Data for summer (DJF), autumn (MAM), winter (JJA), and spring (SON) are plotted with crosses, circles, triangles, and squares, respectively. Data for October 29 to December 23 (OND) are plotted with green diamonds, with the linear least squares fit shown by green dashed lines. DJF, December–January–February; MAM, March–April–May; JJA, June–July–August; SON, September–October–November.

overlapping the period when the significantly positive $\Delta_{DC-DDU}$ values were observed in October–December. This underestimate implies that the model might lack sulfate formation processes that causes $\Delta^{17}O(SO_4^{2-})_{nss}$ of higher than 2.0‰ ± 0.3‰ at the inland site (Table 1) and thus the positive $\Delta_{DC-DDU}$ in this time period. Meanwhile for DDU, the model also underestimates $\Delta^{17}O(SO_4^{2-})_{nss}$ from September to October by 0.6‰–0.8‰, but rather slightly overestimates in January by 0.5‰ (Figure 2d). This result is further discussed in the following sections within the focus of the observed intersite differences.

## 4. Discussion

The $\Delta_{DC-DDU}$ values different from 0‰ during the austral spring to summer (October–December) and during the austral autumn (March–May) (Figure 1d) suggest that some fractions of sulfate existing at these inland and coastal sites experienced different oxidation processes. The possible processes may include long-range transport of sulfate produced above the other continents or in the stratosphere (i.e., nmb-$SO_4^{2-}$), in addition to DMS-sourced sulfate produced within the troposphere above the Antarctic continents and the Southern Ocean. In the former case, it is expected that $\delta^{34}S_{nss}$ values in the same aerosol samples would specifically decrease during the corresponding periods, since nmb-$SO_4^{2-}$ has lower $\delta^{34}S_{nss}$ values than DMS-sourced sulfate (Ishino et al., 2019; Patris et al., 2000; Pruett et al., 2004). Indeed, Ishino et al. (2019) found an unexpected decrease of $\delta^{34}S_{nss}$ at Dome C in November, suggesting a significant input of nmb-$SO_4^{2-}$, which is likely attributed to long-range transport of continental submicron aerosols based on a significant correlation with $^{210}Pb$ tracer. This input of nmb-$SO_4^{2-}$ in November overlaps the period of the positive $\Delta_{DC-DDU}$ values. However, there were not significant correlations observed for the $\Delta_{DC-DDU}$ compared to $\delta^{34}S_{nss}$ ($p = 0.39$) and $^{210}Pb$ ($p = 0.15$) at Dome C (Figures 3a and 3b, and Table S1). Therefore, this nmb-$SO_4^{2-}$ is not likely the main factor causing the positive $\Delta_{DC-DDU}$, while it may dilute or perturb the high $\Delta^{17}O(SO_4^{2-})_{nss}$ signature in that period. Since $\delta^{34}S_{nss}$ values were homogeneous between Dome C and DDU for the rest period of the year (Ishino et al., 2019), the negative $\Delta_{DC-DDU}$ values during the autumn would neither be associated with the contribution of nmb-$SO_4^{2-}$. Additionally, whereas the deposition of polar stratospheric clouds is thought to be a potential source of tropospheric sulfate in Antarctica, it is likely to occur during midwinter (July–August) (Savarino et al., 2007), not coinciding with the positive and negative $\Delta_{DC-DDU}$ values. Furthermore, the relative abundance of $^{35}S$, a radioactive tracer often used as an indicator of stratospheric sulfate, relative to total sulfate is maximized in June (Hill-Falkenthal et al., 2013). Therefore, the intrusion of stratospheric sulfate is not the likely reason for the $\Delta_{DC-DDU}$ values discussed here. Thus, below we discuss possible influences of regional characteristic chemistry taking place at the scale of the Antarctic continent on $\Delta^{17}O(SO_4^{2-})_{nss}$ during these periods.

### 4.1. Positive $\Delta_{DC-DDU}$ Values in Austral Spring–Summer

Positive $\Delta_{DC-DDU}$ in spring–summer coincides with a $[O_3]$ increase from 25 to 34 ppb at Dome C (Figure 1e) and a significant drop of $[MS^-]/[SO_4^{2-}]_{nss}$ ratios at Dome C (Figure 1f) from 0.13 ± 0.04 (October) to 0.05 ± 0.02 (January). $[MS^-]/[SO_4^{2-}]_{nss}$ generally shows a bimodal seasonal cycle with slight increase from winter (July–August; 0.06 ± 0.01) to spring (October; 0.13 ± 0.04), followed by a significant drop in

summer (January; 0.05 ± 0.02) and then increases to maximum values in autumn (March; 0.25 ± 0.09) at Dome C (Legrand, Preunkert, Weller, et al., 2017). Legrand, Preunkert, Weller, et al. (2017) found that the decline of $[MS^-]/[SO_4^{2-}]_{nss}$ during summer coincides with periods of high photochemical activity as indicated by high $O_3$ levels, suggesting the occurrence of chemical destruction of $MS^-$. Legrand, Preunkert, Weller, et al. (2017) also showed that the decrease in $[MS^-]/[SO_4^{2-}]_{nss}$ at DDU is less significant than Dome C, while $MS^-$ destruction may also occur at DDU where is frequently exposed to the highly oxidative atmosphere from the interior Antarctica during summer due to katabatic wind (Legrand, Preunkert, et al., 2016). The cooccurrence of $MS^-$ destruction at Dome C and positive $\Delta_{DC-DDU}$ (Figures 1d and 1f) is striking, suggesting the possibility that $MS^-$ destruction produces sulfate with significantly high $\Delta^{17}O(SO_4^{2-})_{nss}$ at Dome C and leads to the high $\Delta_{DC-DDU}$. This possibility is supported by the negative covariation between the $\Delta_{DC-DDU}$ and $[MS^-]/[SO_4^{2-}]_{nss}$ at Dome C for October–December with $p$ value of 0.01 (Figure 3c and Table S1), where $\Delta_{DC-DDU}$ tends to be higher as $[MS^-]/[SO_4^{2-}]_{nss}$ becomes lower.

This hypothesis requires that $MS^-$ possesses significantly high $\Delta^{17}O$ signature or $MS^-$ destruction occurs via its oxidation by $O_3$ to produce sulfate. It is known that $MS^-$ formation in the MBL involves $O_3$ as well as BrO, which is produced via Br + $O_3$ (Zhang et al., 1997), as important oxidants (Hoffmann et al., 2016; von Glasow & Crutzen, 2004). These oxidants would imprint a high $\Delta^{17}O$ value on $MS^-$. To date, however, there are no observations or estimates of $\Delta^{17}O(MS^-)$. The mechanism and the subsequent products of $MS^-$ destruction in inland Antarctica remain unclear. While $MS^-$ oxidation by OH, $SO_4^-$, Cl, and $Cl_2^-$ has been proposed so far (Zhu, 2004; Zhu et al., 2003a, 2003b), there is no evidence for a reaction with $O_3$. A previous box model study simulating multiphase sulfur chemistry (Hoffmann et al., 2016) indicated that aqueous-phase oxidation of $MS^-$ by OH to produce sulfate (Zhu et al., 2003a) is the dominant pathway under typical pristine MBL conditions (Bräuer et al., 2013). Furthermore, it is also shown by a flow tube chamber experiment that $MS^-$ can be oxidized on deliquesced aerosols to form sulfate, which may lead to shorter lifetime of $MS^-$ than in condensed aqueous phase in MBL (Mungall et al., 2018). Legrand, Preunkert, Weller, et al. (2017) mentioned that, although the chance of aerosol experiencing aqueous-phase chemistry is far lower than in the MBL, far more acidic conditions on the Antarctic Plateau compared to the MBL would favor the production of OH via the reaction of $O_3$ with $O_2^-$ (Ervens et al., 2003). Thus, here, we assume $MS^-$ oxidation by OH in aqueous phase or on aerosols as the mechanism for $MS^-$ destruction, and for the first time estimate $\Delta^{17}O$ transferred from DMS oxidation to $MS^-$ and then to sulfate.

Figure 4 summarizes the hypothesized sulfate formation processes via $MS^-$ oxidation possibly transferring high $\Delta^{17}O$ to sulfate, in addition to the recognized processes explained in Section 2.4. The reaction scheme includes DMS oxidation into dimethyl sulfoxide (DMSO; $CH_3S(O)CH_3$), methyl sulfinic acid (MSIA; $CH_3S(O)OH$), and then to $MS^-$, as well as production of $SO_2$ from each species, whose importance in the MBL is recognized (Barnes et al., 2006; Chen et al., 2018; Hoffmann et al., 2016; von Glasow & Crutzen, 2004). Note that gas-phase and aqueous-phase reactions using the same oxidants are considered as one pathway for simplification, since they will result in the same $\Delta^{17}O(SO_4^{2-})$. We also summarize the formula for calculating the $\Delta^{17}O$ value of each sulfur species $X$ (DMSO, MSIA, $MS^-$, and $SO_4^{2-}$) produced by each reaction $j$ ($\Delta^{17}O(X)_j$) in Table 2, which is determined based on mechanisms of respective oxidation pathways as follows.

At the first step, DMS oxidation into DMSO includes four different oxidation pathways reacting with OH, BrO, $O_3$, and Cl. These reactions generally occur through adduct of the oxidant to the sulfur atom of DMS (Barnes et al., 2006; Gershenzon et al., 2001; Ingham et al., 1999), transferring oxygen atoms of oxidants to the produced DMSO. Therefore, the $\Delta^{17}O$ transferred to DMSO via DMS + OH, DMS + BrO, and DMS + $O_3$ reflect $\Delta^{17}O$ values of each oxidant. $\Delta^{17}O$ of DMSO produced via DMS + OH is assumed to be equal to $\Delta^{17}O$ of OH, that is, 0‰. Since $^{17}O$-excess is located at the two terminal O-atoms of $O_3$ ($O_3$-terminal) (Bhattacharya et al., 2008; Janssen & Tuzson, 2006), $\Delta^{17}O(O_3)_{term}$ is assumed to be 38.4‰ ± 2.0‰ (=3/2 × $\Delta^{17}O(O_3)_{bulk}$). In addition, BrO receives $O_3$-terminal via Br + $O_3$ (Zhang et al., 1997). DMS + $O_3$ and DMS + BrO are thus expected to produce DMSO with $\Delta^{17}O$ of 39‰. Since DMS + Cl pathway is expected to form $CH_3S(Cl)CH_3$, which is followed by subsequent oxidation by $O_2$ (Barnes et al., 2006), $\Delta^{17}O_{DMS+Cl}$ is assumed to be equal to $\Delta^{17}O(O_2)$ (=−0.3‰; Barkan & Luz, 2005). During DMSO oxidation by OH into MSIA, one of the two oxygen atoms of produced MSIA is from DMSO while another comes from OH (Bardouki et al., 2002), suggesting that $\Delta^{17}O(MSIA)_{DMSO+OH}$ is determined as the sum of $1/2\Delta^{17}O(DMSO)$ and $1/2\Delta^{17}O(OH)$. MSIA is oxidized into $MS^-$ by OH or $O_3$. In MSIA + OH, O-atom added to $MS^-$ is assumed to come from OH, since

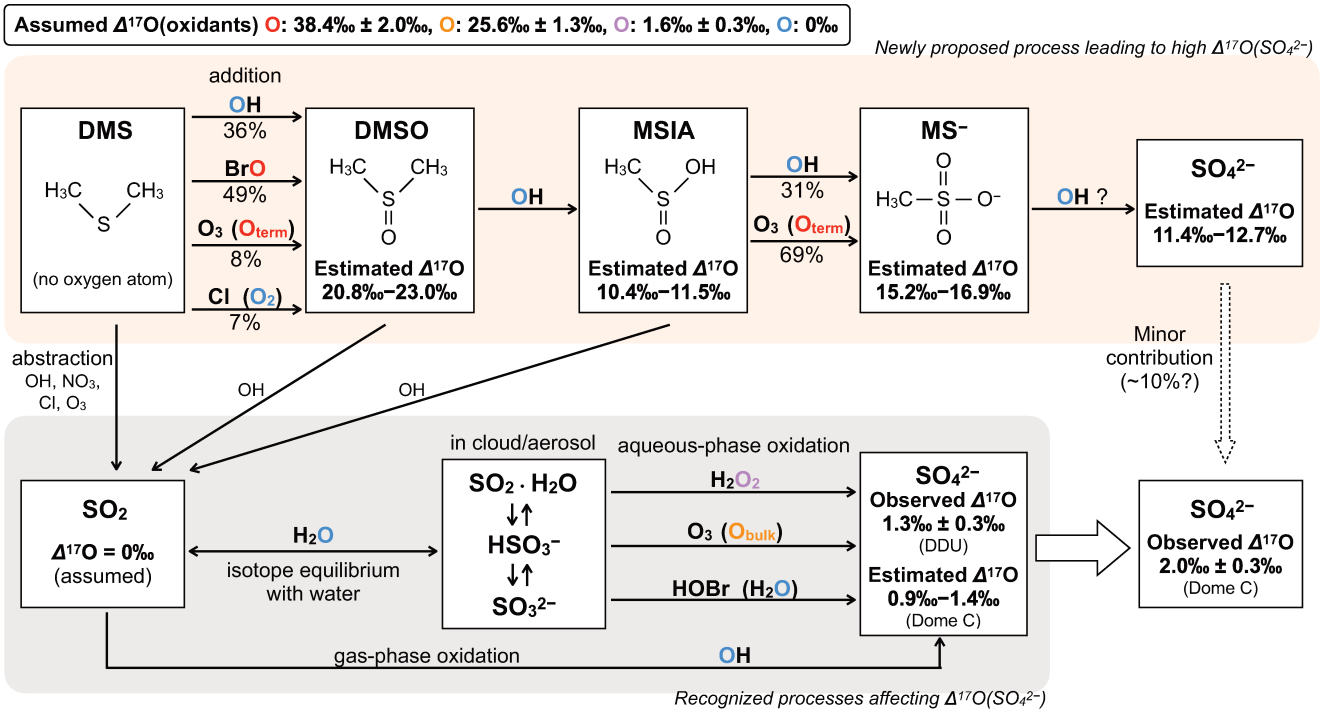


**Figure 4.** Schematic of sulfate formation processes affecting $\Delta^{17}O(SO_4^{2-})_{nss}$ considered in this study. The processes in upper row (orange shaded) are described in Section 4.1, whereas those in lower row (gray shaded) are described in Section 2.4. The $\Delta^{17}O$ of oxidants are indicated by different colors. The $\Delta^{17}O$ of sulfur species shown in the figure represent the mean values for October–December. The percentages shown under arrows are the relative contributions of each pathway averaged within the troposphere in 60°–90°S during October–December, which are estimated by the model with detailed DMS chemistry by Chen et al. (2018). DMS, dimethyl sulfide.

OH is added to S-atom of MSIA to form $CH_3S(O)(OH)_2$ adduct before its reaction with $O_2$ to form $MS^-$ (Bardouki et al., 2002). In MSIA + $O_3$, it is experimentally indicated that $O_3$-terminal transfers to $MS^-$ (Flyunt et al., 2001). In both reactions, two of three O-atoms of $MS^-$ are preserved from MSIA. Therefore, $\Delta^{17}O$ transferring to $MS^-$ via each reaction is determined as sum of $2/3\Delta^{17}O(MSIA)$ and $1/3\Delta^{17}O(oxidant)$. Finally, assuming $MS^-$ + OH provides one O-atom from OH to produce sulfate, $\Delta^{17}O(MS^-)_{MS+OH}$ is determined as the sum of $3/4\Delta^{17}O(MS^-)$ and $1/4\Delta^{17}O(OH)$ (Table 2).

With the above assumptions on $\Delta^{17}O$ transferring processes, $\Delta^{17}O$ value of species $X$ is determined by the isotopic mass balance as the following equation:

$$\Delta^{17}O(X) = \sum \Delta^{17}O(X)_j \, f_j, \tag{6}$$

**Table 2**
*Expected $\Delta^{17}O$ Values of Sulfur Species Produced Through Oxidation of DMS From Different Reaction Mechanisms*

| Reaction | $\Delta^{17}O(X)_j$ | Reference |
|---|---|---|
| DMS + OH (add) | $\Delta^{17}O(DMSO)_{DMS+OH} = \Delta^{17}O(OH)$ | Barnes et al. (2006) |
| DMS + BrO | $\Delta^{17}O(DMSO)_{DMS+BrO} = \Delta^{17}O(BrO) = \Delta^{17}O(O_3)_{term}$ | Ingham et al. (1999) |
| DMS + $O_3$ | $\Delta^{17}O(DMSO)_{DMS+O_3} = \Delta^{17}O(O_3)_{term}$ | Gershenzon et al. (2001) |
| DMS + Cl (+$O_2$) | $\Delta^{17}O(DMSO)_{DMS+Cl} = \Delta^{17}O(O_2)$ | Barnes et al. (2006) |
| DMSO + OH | $\Delta^{17}O(MSIA)_{DMSO+OH} = 1/2\Delta^{17}O(DMSO) + 1/2\Delta^{17}O(OH)$ | Wang and Zhang (2002) |
| MSIA + OH | $\Delta^{17}O(MS^-)_{MSIA+OH} = 2/3\Delta^{17}O(MSIA) + 1/3\Delta^{17}O(OH)$ | González-García et al. (2007); Tian et al. (2007) |
| MSIA + $O_3$ | $\Delta^{17}O(MS^-)_{MSIA+O_3} = 2/3\Delta^{17}O(MSIA) + 1/3\Delta^{17}O(O_3)_{term}$ | Flyunt et al. (2001); Kukui et al. (2000) |
| $MS^-$ + OH | $\Delta^{17}O(SO_4^{2-})_{MS+OH} = 3/4\Delta^{17}O(MS^-) + 1/4\Delta^{17}O(OH)$ | Zhu et al. (2003a); Hoffmann et al. (2016) |

$$f_j = P(X)_j / \sum P(X)_j, \quad (7)$$

where $f_j$ is relative contribution of reaction $j$ for production of $X$ ($P(X)$). To obtain $\Delta^{17}O(MS^-)$, we here used $P(X)_j$ and thus $f_j$ estimated by the previous simulation using GEOS-Chem by Chen et al. (2018), which incorporated whole sulfur chemistry shown in Figure 4. We used the mean $P(X)_j$ within the troposphere in 60°–90°S during October–December. For production of DMSO, $f_{DMS+OH}$, $f_{DMS+BrO}$, $f_{DMS+O_3}$, and $f_{DMS+Cl}$ are estimated to be 36%, 49%, 8%, and 7%, respectively. By applying these estimated $f_j$ with $\Delta^{17}O(X)_j$ defined in Table 2 and Equation 6, the $\Delta^{17}O(DMSO)$ is estimated to be 20.8‰–23.0‰. Since MSIA production occurs via DMSO + OH only ($f_{DMSO+OH} = 100\%$), $\Delta^{17}O(MSIA)$ is equivalent to $\Delta^{17}O(MSIA)_{DMSO+OH}$ = 10.4‰–11.5‰. For production of $MS^-$, $f_{MSIA+OH}$ and $f_{MSIA+O_3}$ are estimated to be 31% and 69%, respectively, consequently leading to $\Delta^{17}O(MS^-)$ of 15.2‰–16.9‰. Finally, $\Delta^{17}O(SO_4^{2-})$ derived via $MS^-$ destruction, $\Delta^{17}O_{MS+OH}$, is estimated to be 11.4‰–12.7‰.

If the oxidation of $MS^-$ into sulfate fully corresponds to the difference in $[MS^-]/[SO_4^{2-}]_{nss}$ of 0.09 between Dome C (0.05 ± 0.02) and DDU (0.14 ± 0.07) during October–December, $\Delta^{17}O(SO_4^{2-})_{nss}$ can increase by 1.1‰ (=$\Delta^{17}O(SO_4^{2-})_{MS+OH} \times 0.09$), which is close to the observed $\Delta_{DC-DDU}$ of about 0.7‰. Additionally, the intercept of the slope of $\Delta_{DC-DDU}$ versus $[MS^-]/[SO_4^{2-}]_{nss}$ relationship (Figure 3) suggests that $\Delta^{17}O(SO_4^{2-})_{nss}$ can increase by 1.6‰ if all $MS^-$ observed at DDU was converted to sulfate at Dome C (i.e., $[MS^-]/[SO_4^{2-}]_{nss}$ decreases from 0.14 ± 0.07 to 0), which is consistent with $\Delta^{17}O(SO_4^{2-})_{MS+OH} \times 0.14 \pm 0.07 = 1.7‰ \pm 0.9‰$. These consistencies imply that the positive $\Delta_{DC-DDU}$ observed in the austral spring–summer is mainly caused by $MS^-$ destruction. We therefore conclude that $MS^-$ destruction and subsequent sulfate production along with transport over the Antarctic Plateau is the most likely process responsible for the positive $\Delta_{DC-DDU}$ in the austral spring–summer at inland Antarctica.

The model underestimate of $\Delta^{17}O(SO_4^{2-})_{nss}$ for Dome C during August–December by 0.5‰–1.1‰ (Figure 2c) is also within the possible range of the expected shift in $\Delta^{17}O(SO_4^{2-})_{nss}$ by $MS^-$ destruction, that is, 1.6‰ at maximum (Figure 3). Note that the $MS^-$ destruction becomes significant from November (Figure 1f), only for the latter period of this underestimate of $\Delta^{17}O(SO_4^{2-})_{nss}$ in the model. Additionally, the model also underestimates $\Delta^{17}O(SO_4^{2-})_{nss}$ for DDU during September–October by 0.6‰–0.8‰, while does not during November–December. The absence of $\Delta^{17}O(SO_4^{2-})_{nss}$ underestimate for DDU during November–December is expected because $MS^-$ destruction in the midsummer is less significant at DDU than Dome C (Legrand, Preunkert, Weller, et al., 2017). On the other hand, the underestimates of $\Delta^{17}O(SO_4^{2-})_{nss}$ in early spring at both sites indicate the other missing processes such that impacts both sites. One idea that might cause the underestimates of $\Delta^{17}O(SO_4^{2-})_{nss}$ is the underestimates of $F_{S(IV)+O_3}$ due to the excessive sulfur loading (Figures 2a and 2b). Since S(IV) + $O_3$ reaction prefers higher pH condition, the excessive acidification of cloud water and sea-salt aerosols induced by the overestimates of $[SO_4^{2-}]_{nss}$ may result in suppression of S(IV) + $O_3$. This idea is uncertain because the overestimate of $[SO_4^{2-}]_{nss}$ is not specific for early spring but seen for year round. Additionally, there remains possibility that $\Delta^{17}O(OH)$ is higher than 3‰ (Savarino et al., 2016), that might partially correspond to the underestimates in $\Delta^{17}O(SO_4^{2-})_{nss}$. Future modeling work incorporating DMSO, MSIA, $MS^-$, and sulfate possessing different $\Delta^{17}O$ signatures is necessary to examine if this underestimate in $\Delta^{17}O(SO_4^{2-})_{nss}$ at Dome C corresponds to the lack of $MS^-$ destruction in the model.

This finding that confirms the suspected occurrence of an efficient atmospheric oxidation of $MS^-$ into sulfate over the Antarctic Plateau has an important implication for the interpretation of ice core $\Delta^{17}O(SO_4^{2-})_{nss}$ records. Previous studies revealed that, in Antarctica, $MS^-$ in snow is largely lost after deposition (Delmas et al., 2003; Wagnon et al., 1999; Weller et al., 2004). While the mechanism of this $MS^-$ loss in snow is under debated, there are two proposed ideas: physical migration of $MS^-$ within firn layers and possibly by $MS^-$ oxidation by OH in quasi-brine layer of snow grain. If being viable, the latter $MS^-$ oxidation should increase $\Delta^{17}O(SO_4^{2-})_{nss}$ values in snow after deposition of $MS^-$ and sulfate. Indeed, the previous measurements of $\Delta^{17}O(SO_4^{2-})_{nss}$ in Antarctic ice corresponding to the present-day warm climate period (Holocene) average 2.8‰ ± 0.4‰ (Alexander et al., 2002, 2003; Kunasek et al., 2010; Sofen et al., 2014), which is significantly higher than the annual mass-weighted average of $\Delta^{17}O(SO_4^{2-})_{nss}$ of 1.7‰ ± 0.1‰ in aerosols at Dome C (Table 1). Even the maximum monthly mean $\Delta^{17}O(SO_4^{2-})_{nss}$ of 2.5‰ ± 0.1‰ in July cannot reach the ice core $\Delta^{17}O(SO_4^{2-})_{nss}$ of 2.8‰ ± 0.4‰, indicating the additional sulfate production with the higher $\Delta^{17}O$

$(SO_4^{2-})_{nss}$ in snow after deposition. The degree of postdepositional loss of $MS^-$ tends to be higher at sites with lower snow accumulation rates (Delmas et al., 2003) and reaches 80%–90% at Vostok where the present-day snow accumulation rate is 2.2 g $cm^{-2}$ $year^{-1}$ (Wagnon et al., 1999). Assuming 90% of $MS^-$ in snow is converted into sulfate at Dome C where the accumulation rate (2.7 g $cm^{-2}$ $year^{-1}$) is similar to the one in Vostok, combined with the annual mean $[MS^-]/[SO_4^{2-}]_{nss}$ in aerosols of 0.11 (Legrand, Preunkert, Weller, et al., 2017), $\Delta^{17}O(SO_4^{2-})_{nss}$ can increase by 1.1‰–1.3‰ ($=\Delta^{17}O(SO_4^{2-})_{MS+OH} \times 0.11 \times 0.9$) at maximum. This estimated postdepositional shift in $\Delta^{17}O(SO_4^{2-})_{nss}$ is in agreement with the difference between atmosphere and snow $\Delta^{17}O(SO_4^{2-})_{nss}$, indicating the significance of the postdepositional oxidation of $MS^-$ to sulfate as a controlling factor of ice core $\Delta^{17}O(SO_4^{2-})_{nss}$. Thus, we argue that, to use ice core $\Delta^{17}O(SO_4^{2-})_{nss}$ for assessing past atmospheric oxidant chemistry, it is necessary to correct the ice core $\Delta^{17}O(SO_4^{2-})_{nss}$ for this process. For this purpose, the investigation of the relationship between $\Delta^{17}O(SO_4^{2-})_{nss}$ and $[MS^-]/[SO_4^{2-}]_{nss}$ in snow at various sites with different snow accumulation rates over Antarctica will be required as a future step. Additionally, observations of $\Delta^{17}O(MS^-)$ in aerosols, snow, and ice will provide useful information to prove the proposed mechanisms as well as to constrain the sulfur chemistry in atmospheric chemical-transport models.

### 4.2. Negative $\Delta_{DC-DDU}$ Values in Austral Autumn

The negative $\Delta_{DC-DDU}$ values ranging −1.4‰ ± 0.6‰ to −0.5‰ ± 0.3‰ were observed in austral autumn (March–May) (Figure 1d), suggesting that sulfate with higher $\Delta^{17}O(SO_4^{2-})_{nss}$ is produced at or transported to DDU, compared to Dome C. The largest negative $\Delta_{DC-DDU}$ value of −1.4‰ ± 0.6‰ was observed in April. Meanwhile, the model in the present study slightly underestimates the observed $\Delta^{17}O(SO_4^{2-})_{nss}$ at DDU in April (modeled: 1.6‰–2.1‰, observed: 2.4 ± 0.5‰) but reproduces the observed $\Delta^{17}O(SO_4^{2-})_{nss}$ at Dome C (modeled: 1.7‰–2.1‰, observed: 1.7 ± 0.1‰) within the range of standard deviation of observations (Figure 2). Below, we consider processes that possibly lead to high $\Delta^{17}O(SO_4^{2-})_{nss}$ at DDU in this period and that also can explain the underestimate of $\Delta^{17}O(SO_4^{2-})_{nss}$ at DDU in the model.

The negative $\Delta_{DC-DDU}$ values in March–May coincide with the period when $[Br_y^*]$ is minimal at both sites (Figure 1g). This $[Br_y^*]$ minimum in autumn is thought to be a result of the decrease in $Br_y$ emission from sea salt provided from both open ocean and sea-ice related process (Legrand, Yang, et al., 2016). Since $Br_y^*$ includes HOBr that reacts with S(IV) to produce sulfate with $\Delta^{17}O(SO_4^{2-}) = 0‰$ as mentioned in Section 2.4, the decrease in $[Br_y^*]$ may cause the reduction of $F_{S(IV)+HOBr}$ and the increase in $\Delta^{17}O(SO_4^{2-})_{nss}$. Since $Br_y^*$ emission sources are close to coastal regions, the decrease of $[Br_y^*]$ during autumn compared to the other period is larger at DDU (4.7 ± 1.7 ng $m^{-3}$ for MAM compared to 8.9 ± 1.8 ng $m^{-3}$ for JJA) than Dome C (1.0 ± 0.4 ng $m^{-3}$ for MAM compared to 1.9 ± 0.8 ng $m^{-3}$ for JJA). Given the larger decrease of $[Br_y^*]$ at DDU than Dome C during autumn, it seems that $F_{S(IV)+HOBr}$ might decrease and $\Delta^{17}O(SO_4^{2-})_{nss}$ might increase at larger degree at DDU than Dome C, resulting in the negative $\Delta_{DC-DDU}$ values. However, although the model also shows the larger decrease in $[Br_y^*]$ during autumn at DDU (3.5 ± 1.4 ng $m^{-3}$ for MAM compared to 12.8 ± 2.7 ng $m^{-3}$ for JJA) than Dome C (5.1 ± 1.4 ng $m^{-3}$ for MAM compared to 2.2 ± 0.5 ng $m^{-3}$ for JJA) (Figure S1), the change in the modeled $F_{S(IV)+HOBr}$ was smaller at DDU (23% for MAM compared to 33% for JJA) than Dome C (18% for MAM compared to 33% for JJA) (Table 1). Therefore, the larger decrease in $[Br_y^*]$ at DDU than Dome C does not lead to a larger decrease in $F_{S(IV)+HOBr}$ at DDU in the model. Furthermore, despite the good reproducibility of $[Br_y^*]$ at DDU during MAM by the model (observed: 4.7 ± 1.7 ng $m^{-3}$, modeled: 3.5 ± 1.4 ng $m^{-3}$), the model tends to underestimate tropospheric BrO vertical column density in 60°–90°S during March–April by a factor of ~4 (Figure S2), implying that the model could also underestimate HOBr abundance. The underestimate of HOBr abundance would lead to underestimate of $F_{S(IV)+HOBr}$ and overestimate of $\Delta^{17}O(SO_4^{2-})_{nss}$, which is opposed to the obtained result of underestimate in $\Delta^{17}O(SO_4^{2-})_{nss}$ during autumn at DDU. Rather, given that BrO in 60°–90°S is underestimated year round (Figure S2), it could be a reason for overestimate of $\Delta^{17}O(SO_4^{2-})_{nss}$ such that seen for DDU in January (Figure 2d). We note that, based on the kinetics of $HSO_3^-$ + HOCl investigated by a flow tube experiment, Liu and Abbatt (2020) recently determined reaction rate constant of $HSO_3^-$ + HOBr ($k_{HOBr+HSO_3^-}$) which was estimated to be 2 orders of magnitude lower than the values used in atmospheric models including GEOS-Chem. However, Chen et al. (2017) had performed a sensitivity test with the 2 orders

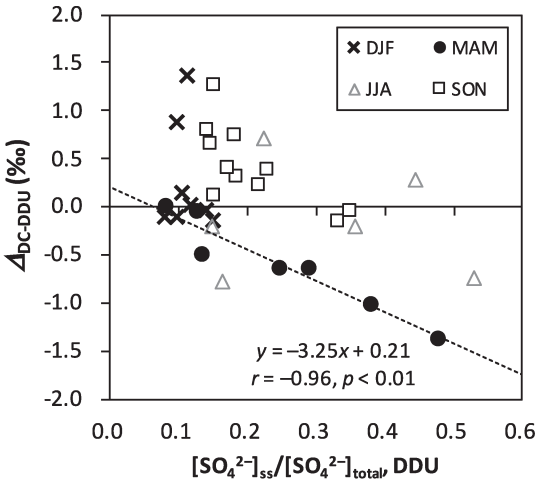


**Figure 5.** Relationship between $[SO_4^{2-}]_{ss}/[SO_4^{2-}]_{total}$ at DDU and $\Delta_{DC-DDU}$. Symbols for different seasons are same as Figure 3. The dashed line shows the linear least squares fit for autumn (MAM). DDU, Dumont d'Urville; MAM, March–April–May.

of magnitude lower $k_{HOBr+HSO_3^-}$ and showed that the contribution of S(IV) + HOBr reaction to the global sulfate formation does not change because this reaction is limited by gas diffusion of HOBr into cloud droplets. Thus, it seems that the current understanding in S(IV) + HOBr pathway and related reactive bromine chemistry cannot explain the underestimate of $\Delta^{17}O(SO_4^{2-})_{nss}$ at DDU during the autumn in the model.

Another possible explanation is the increase in $\Delta^{17}O(SO_4^{2-})_{nss}$ at DDU associated with the aqueous-phase S(IV) + $O_3$ pathway in sea-salt aerosol. As mentioned in Section 2.3, fresh sea salts typically contain alkaline solution (pH ~ 8) where the S(IV) + $O_3$ pathway is efficient prior to aerosol acidification (Alexander et al., 2005). It is thus expected that, while sea-salt loading in autumn (0.9 ± 0.4 μg $m^{-3}$ for MAM) is lower than in summer (1.1 ± 0.4 μg $m^{-3}$ for DJF) by only a factor of 1.2, the $[SO_4^{2-}]_{nss}$ level in autumn (57 ± 46 ng $m^{-3}$) is a factor of 4 lower than that in summer (215 ± 79 ng $m^{-3}$), leading to slower sea-salt acidification, possibly allowing S(IV) + $O_3$ to proceed. This possibility seems to be supported by the negative covariation between the $\Delta_{DC-DDU}$ and $[SO_4^{2-}]_{ss}/[SO_4^{2-}]_{total}$ at DDU, an assumed index of the degree of sea-salt acidification, for the data during March to May with $r = -0.96$ and $p < 0.01$ (Figure 5 and Table S1), where the $\Delta_{DC-DDU}$ tends to be lower as $[SO_4^{2-}]_{ss}/[SO_4^{2-}]_{total}$ becomes higher. Note that, however, since both $\Delta^{17}O(SO_4^{2-})_{nss}$ and $[SO_4^{2-}]_{ss}/[SO_4^{2-}]_{total}$ are determined as functions of $k \times [Na^+]$ in Equation 1, the correlation between the $\Delta_{DC-DDU}$ and $[SO_4^{2-}]_{ss}/[SO_4^{2-}]_{total}$ could be an artifact of the calculation. If we assume $[Na^+]/[SO_4^{2-}]_{total}$ as an index of sea-salt loading relative to titrating acids without using $k$ value, the correlation coefficient compared to $\Delta_{DC-DDU}$ becomes less significant ($r = -0.74$ and $p = 0.06$; Table S1). Hence, it is currently difficult to conclude the role of sea salt controlling $\Delta^{17}O(SO_4^{2-})_{nss}$ and $\Delta_{DC-DDU}$ values based on the available data. In the meantime, the sea-salt aerosol in the model may be acidified excessively because of the overestimate of $[SO_4^{2-}]_{nss}$ (Figures 2a and 2b), while the model fairly reproduces the abundances of sea-salt aerosols at DDU by implementing sea-salts production from blowing snow sublimation (Huang & Jaeglé, 2017; Figure S1). The excessive acidification of sea salt in the model would lead to the underestimate of $F_{S(IV)+O_3}$ and then $\Delta^{17}O(SO_4^{2-})_{nss}$. Therefore, the small underestimate of $\Delta^{17}O(SO_4^{2-})_{nss}$ at DDU during autumn might be partly compensated by correcting $[SO_4^{2-}]_{nss}$.

In both cases, to obtain the negative $\Delta_{DC-DDU}$ values, sulfate with high $\Delta^{17}O(SO_4^{2-})_{nss}$ of 1.9‰ ± 0.2‰ during autumn at DDU needs to be reduced and sulfate with lower $\Delta^{17}O(SO_4^{2-})_{nss}$ needs to be increased along with the transport of sulfate and its precursors toward inland Antarctica. It is reasonable that, since liquid water content becomes zero at −40°C (Jeffery & Austin, 1997; Pruppacher, 1995), aqueous-phase S(IV) oxidation is strictly limited and sulfate produced via gas-phase $SO_2$ + OH pathway with $\Delta^{17}O(SO_4^{2-})_{nss} = 0‰$ is more important at inland Antarctica, represented by Dome C where the annual mean temperature is −50°C (Argentini et al., 2014). Additionally, given that $[Na^+]$ is 2 orders of magnitude lower at Dome C (ca., 5 ng $m^{-3}$; Legrand, Preunkert, Wolff, et al., 2017) than DDU (ca., 300 ng $m^{-3}$; Jourdain & Legrand, 2002), it is expected that the sea-salt particles preferentially deposit during transport toward inland Antarctica together with sulfate produced in sea salt, possibly leading to sulfate with lower $\Delta^{17}O(SO_4^{2-})_{nss}$ values at Dome C. Thus, it seems qualitatively reasonable to observe lower $\Delta^{17}O(SO_4^{2-})_{nss}$ at Dome C than DDU.

Thus, the changes in sulfate formation processes responsible for the negative $\Delta_{DC-DDU}$ values during March–May are uncertain. Considering the small but significant underestimate in $\Delta^{17}O(SO_4^{2-})_{nss}$ at DDU in the model despite of the good reproducibility at Dome C in that period, we looked into the processes that would be more important around coastal regions than inland such as the decrease in $F_{S(IV)+HOBr}$ and the increase in $F_{S(IV)+O_3}$ in sea-salt particles at DDU. However, both of them are not decisive. Given the larger abundances of reactive bromine at coastal regions of West Antarctica than those of East Antarctica (Grilli et al., 2013; Saiz-Lopez et al., 2007; Theys et al., 2011), further observations of $\Delta^{17}O(SO_4^{2-})_{nss}$ at different coastal sites around Antarctica would help to constrain the importance of those processes.

## 5. Conclusions

We investigated the consequences of characteristic oxidation chemistry in Antarctica for sulfate formation processes and $\Delta^{17}O(SO_4^{2-})_{nss}$ by comparing weekly $\Delta^{17}O(SO_4^{2-})_{nss}$ observations at inland site Dome C and those previously obtained at coastal site DDU in the same year 2011. The $\Delta^{17}O(SO_4^{2-})_{nss}$ at Dome C showed lower values in austral summer (1.1‰ ± 0.1‰ in February) and higher values in winter (2.5‰ ± 0.2‰ in August), with a mass-weighted annual average of 1.7‰ ± 0.1‰, which are generally consistent with previous observations at DDU. This seasonality in $\Delta^{17}O(SO_4^{2-})_{nss}$ at Dome C is roughly reproduced by the GEOS-Chem atmospheric chemistry transport model, reflecting the increased relative fraction of sulfate produced via $SO_2$ + OH (34%) and S(IV) + $H_2O_2$ (48%) in summer in contrast to the increased fraction of S(IV) + $O_3$ (30%) and S(IV) + HOBr (34%) in winter. The model also reproduces the $\Delta^{17}O(SO_4^{2-})_{nss}$ at DDU with estimated sulfate formation processes similar to Dome C but with lower fraction of gas-phase OH oxidation for DDU (16% in summer).

Aside from those general seasonal trends, we found that there are significant differences in $\Delta^{17}O(SO_4^{2-})_{nss}$ at Dome C and DDU during the austral spring–summer (October–December) and the austral autumn (March–May), indicating the contribution of specific oxidation chemistry to sulfate at each site. For spring–summer, the higher $\Delta^{17}O(SO_4^{2-})_{nss}$ at Dome C than DDU was observed, which coincides with the period when chemical $MS^-$ destruction is enhanced under the high photochemical activity at Dome C. Combined with the first estimate of $\Delta^{17}O(MS^-)$ based on the isotopic mass balance calculations, we conclude that $MS^-$ destruction producing sulfate with $\Delta^{17}O(SO_4^{2-})_{nss}$ as high as 12‰ is the most likely process responsible for the observed high $\Delta^{17}O(SO_4^{2-})_{nss}$ at Dome C and suggests that $MS^-$ destruction is responsible for about 10% of total sulfate during spring–summer at this inland Antarctic location. This finding has important implications for the interpretation of ice core $\Delta^{17}O(SO_4^{2-})_{nss}$ records, since it is known that $MS^-$ can be also chemically destroyed in snow. This process may lead to a significant postdepositional increase in $\Delta^{17}O(SO_4^{2-})_{nss}$ of over 1‰ and reconcile the existing discrepancy between the $\Delta^{17}O(SO_4^{2-})_{nss}$ in the atmosphere and ice. For a precise interpretation of ice core $\Delta^{17}O(SO_4^{2-})_{nss}$ records, future works investigating the relationship between $\Delta^{17}O(SO_4^{2-})_{nss}$ and $[MS^-]/[SO_4^{2-}]_{nss}$ in snow at various sites over Antarctica are required to formulate the postdepositional shift of $\Delta^{17}O(SO_4^{2-})_{nss}$. Additionally, the calculation of $\Delta^{17}O(MS^-)$ should be implemented into the model that is used for simulation of the past $\Delta^{17}O(SO_4^{2-})_{nss}$. Developments of analytical methods for $\Delta^{17}O(MS^-)$ are also necessary to prove the proposed mechanisms as well as to constrain the models. Meanwhile, the higher $\Delta^{17}O(SO_4^{2-})_{nss}$ at DDU than Dome C during autumn may be associated with decreased contribution of S(IV) + HOBr due to the limited reactive bromine availability and/or the increased contribution of S(IV) + $O_3$ due to the insufficient acidification of sea salt at DDU. Further observations of $\Delta^{17}O(SO_4^{2-})_{nss}$ at various coastal sites over Antarctica will help to constrain the impact of these processes.

## Conflict of Interest

The authors declare no conflicts of interest.

## Data Availability Statement

Data presented in this article are available at http://dx.doi.org/10.17632/xfr8ffn9xv.1.

**Acknowledgments**
We thank Shuting Zhai for providing support to S.I. and S.H. for handling the GEOS-Chem model. We acknowledge financial supports and field supplies for winter and summer campaigns at Dome C and DDU by the Institut Polaire Français Paul Emile Victor (IPEV) from program 1011 (SUNITEDC) and program 1177 (CAPOXI 35-75). We also thank aerosol data provided via the French Environmental Observation Service CESOA, which was supported by IPEV and the National Institute of Sciences of the Universe (INSU-CNRS). We acknowledge JSPS KAKENHI (JP17J08978 [S.I.], JP19J00682 [S.I.], JP16H05884 [S.H.], JP18H05050 [S.H.], JP20H04305 [S.H.], JP20H04969 [S.H.], and JP17H06105 [N.Y. and S.H.]) from the Ministry of Education, Culture, Sports, Science and Technology (MEXT), Japan. We acknowledge Labex OSUG@2020 (Investissements d'avenir – ANR10 LABX56), the French Agence Nationale de la Recherche (ANR) FOFAMIFS project (grant ANR—14-CE33-0009-01) and EAIIST project (grant ANR—16-CE01-0011-01) (J.S.), NSF AGS award 1343077 and 1702266 (B.A.), and NASA award 80NSSC19K1273 (L.J.). The BNP-Paribas foundation is also acknowledged for its financial support under its climate initiative (J.S.). AppSILAS, a scientific program of LEFE-CHAT from the Institut National des Sciences de l'Univers/CNRS, has also provided partial funding for this study (J.S.). S.H. acknowledges JSPS and CNRS under the JSPS–CNRS Joint Research Program. J.S. acknowledges the CNRS/INSU (PRC program 207394) and the PH-SAKURA program of the French Embassy in Japan (project 31897PM) for financial support. This is publication 3 of PANDA platform. Meteo France is acknowledged for providing meteorological data at DDU and IPEV/PNRA for providing routine meteorological observation at station Concordia (www.climantartide.it).

## References

Alexander, B., Allman, D. J., Amos, H. M., Fairlie, T. D., Dachs, J., Hegg, D. A., & Sletten, R. S. (2012). Isotopic constraints on the formation pathways of sulfate aerosol in the marine boundary layer of the subtropical northeast Atlantic Ocean. *Journal of Geophysical Research*, *117*(6), D06304. https://doi.org/10.1029/2011JD016773

Alexander, B., & Mickley, L. J. (2015). Paleo-perspectives on potential future changes in the oxidative capacity of the atmosphere due to climate change and anthropogenic emissions. *Current Pollution Reports*, *1*, 57–69. https://doi.org/10.1007/s40726-015-0006-0

Alexander, B., Park, R. J., Jacob, D. J., Li, Q. B., Yantosca, R. M., Savarino, J., et al. (2005). Sulfate formation in sea-salt aerosols: Constraints from oxygen isotopes. *Journal of Geophysical Research*, *110*, D10307. https://doi.org/10.1029/2004JD005659

Alexander, B., Savarino, J., Barkov, N. I., Delmas, R. J., & Thiemens, M. H. (2002). Climate driven changes in the oxidation pathways of atmospheric sulfur. *Geophysical Research Letters*, *29*(14), 1685. https://doi.org/10.1029/2002GL014879

Alexander, B., Thiemens, M. H., Farquhar, J., Kaufman, A. J., Savarino, J., & Delmas, R. J. (2003). East Antarctic ice core sulfur isotope measurements over a complete glacial–interglacial cycle. *Journal of Geophysical Research*, *108*(24), 4876. https://doi.org/10.1029/2003JD003513

Argentini, S., Pietroni, I., Mastrantonio, G., Viola, A. P., Dargaud, G., & Petenko, I. (2014). Observations of near surface wind speed, temperature and radiative budget at Dome C, Antarctic Plateau during 2005. *Antarctic Science*, *26*(1), 104–112. https://doi.org/10.1017/S0954102013000382

Bardouki, H., Da Rosa, M. B., Mihalopoulos, N., Palm, W. U., & Zetzsch, C. (2002). Kinetics and mechanism of the oxidation of dimethylsulfoxide (DMSO) and methanesulfinate (MSI-) by OH radicals in aqueous medium. *Atmospheric Environment*, *36*(29), 4627–4634. https://doi.org/10.1016/S1352-2310(02)00460-0

Barkan, E., & Luz, B. (2005). High precision measurements of $^{17}O/^{16}O$ and $^{18}O/^{16}O$ ratios in $H_2O$. *Rapid Communications in Mass Spectrometry*, *19*(24), 3737–3742. https://doi.org/10.1002/rcm.2250

Barnes, I., Hjorth, J., & Mihalopoulos, N. (2006). Dimethyl sulfide and dimethyl sulfoxide and their oxidation in the atmosphere. *Chemical Reviews*, *106*(3), 940–975. https://doi.org/10.1021/CR020529+

Bhattacharya, S. K., Pandey, A., & Savarino, J. (2008). Determination of intramolecular isotope distribution of ozone by oxidation reaction with silver metal. *Journal of Geophysical Research*, *113*, D03303. https://doi.org/10.1029/2006JD008309

Bräuer, P., Tilgner, A., Wolke, R., & Herrmann, H. (2013). Mechanism development and modeling of tropospheric multiphase halogen chemistry: The CAPRAM Halogen Module 2.0 (HM2). *Journal of Atmospheric Chemistry*, *70*(1), 19–52. https://doi.org/10.1007/s10874-013-9249-6

Chen, Q., Geng, L., Schmidt, J., Xie, Z., Kang, H., Dachs, J., et al. (2016). Isotopic constraints on the role of hypohalous acids in sulfate aerosol formation in the remote marine boundary layer. *Atmospheric Chemistry and Physics*, *16*(17), 11433–11450. https://doi.org/10.5194/acp-16-11433-2016

Chen, Q., Schmidt, J. A., Shah, V., Jaeglé, L., Sherwen, T., & Alexander, B. (2017). Sulfate production by reactive bromine: Implications for the global sulfur and reactive bromine budgets. *Geophysical Research Letters*, *44*, 7069–7078. https://doi.org/10.1002/2017GL073812

Chen, Q., Sherwen, T., Evans, M., & Alexander, B. (2018). DMS oxidation and sulfur aerosol formation in the marine troposphere: A focus on reactive halogen and multiphase chemistry. *Atmospheric Chemistry and Physics*, *18*(18), 13617–13637. https://doi.org/10.5194/acp-18-13617-2018

Cosme, E., Hourdin, F., Genthon, C., & Martinerie, P. (2005). Origin of dimethylsulfide, non-sea-salt sulfate, and methanesulfonic acid in eastern Antarctica. *Journal of Geophysical Research*, *110*, D03302. https://doi.org/10.1029/2004JD004881

Crawford, J. H., Davis, D. D., Chen, G., Buhr, M., Oltmans, S., Weller, R., et al. (2001). Evidence for photochemical production of ozone at the South Pole surface. *Geophysical Research Letters*, *28*(19), 3641–3644. https://doi.org/10.1029/2001GL013055

Davis, D. D., Seelig, J., Huey, G., Crawford, J., Chen, G., & Wang, Y. (2008). A reassessment of Antarctic plateau reactive nitrogen based on ANTCI 2003 airborne and ground based measurements. *Atmospheric Environment*, *42*(12), 2831–2848. https://doi.org/10.1016/j.atmosenv.2007.07.039

Delmas, R. J., Wagnon, P., Goto-Azuma, K., Kamiyama, K., & Watanabe, O. (2003). Evidence for the loss of snow-deposited MSA to the interstitial gaseous phase in central Antarctic firn. *Tellus Series B: Chemical and Physical Meteorology*, *55*(1), 71–79. https://doi.org/10.3402/tellusb.v55i1.16355

Dubey, M. K., Mohrschladt, R., Donahue, N. M., & Anderson, J. G. (1997). Isotope specific kinetics of hydroxyl radical (OH) with water ($H_2O$): Testing models of reactivity and atmospheric fractionation. *Journal of Physical Chemistry A*, *101*(8), 1494–1500. https://doi.org/10.1021/jp962332p

Elsässer, C., Wagenbach, D., Weller, R., Auer, M., Wallner, A., & Christl, M. (2011). Continuous 25-yr aerosol records at coastal Antarctica: Part 2: Variability of the radionuclides $^{7}Be$, $^{10}Be$ $^{210}Pb$. *Tellus Series B: Chemical and Physical Meteorology*, *63*(5), 920–934. https://doi.org/10.1111/j.1600-0889.2011.00543.x

Erbland, J., Vicars, W. C., Savarino, J., Morin, S., Frey, M. M., Frosini, D., et al. (2013). Air–snow transfer of nitrate on the East Antarctic Plateau—Part 1: Isotopic evidence for a photolytically driven dynamic equilibrium in summer. *Atmospheric Chemistry and Physics*, *13*(13), 6403–6419. https://doi.org/10.5194/acp-13-6403-2013

Ervens, B., George, C., Williams, J. E., Buxton, G. V., Salmon, G. A., Bydder, M., et al. (2003). CAPRAM 2.4 (MODAC mechanism): An extended and condensed tropospheric aqueous phase mechanism and its application. *Journal of Geophysical Research*, *108*(14), 4426. https://doi.org/10.1029/2002JD002202

Flyunt, R., Makogon, O., Schuchmann, M. N., Asmus, K. D., & Von Sonntag, C. (2001). OH-radical-induced oxidation of methanesulfinic acid. The reactions of the methanesulfonyl radical in the absence and presence of dioxygen. *Journal of the Chemical Society, Perkin Transactions*, *2*(5), 787–792. https://doi.org/10.1039/b009631h

Fogelman, K. D., Walker, D. M., & Margerum, D. W. (1989). Non-metal redox kinetics: Hypochlorite and hypochlorous acid reactions with sulfite. *Inorganic Chemistry*, *28*(6), 986–993. https://doi.org/10.1021/ic00305a002

Frey, M. M., Savarino, J., Morin, S., Erbland, J., & Martins, J. M. F. (2009). Photolysis imprint in the nitrate stable isotope signal in snow and atmosphere of East Antarctica and implications for reactive nitrogen cycling. *Atmospheric Chemistry and Physics*, *9*(22), 8681–8696. https://doi.org/10.5194/acp-9-8681-2009

Geng, L., Schauer, A. J., Kunasek, S. A., Sofen, E. D., Erbland, J., Savarino, J., et al. (2013). Analysis of oxygen-17 excess of nitrate and sulfate at sub-micromole levels using the pyrolysis method. *Rapid Communications in Mass Spectrometry*, *27*(21), 2411–2419. https://doi.org/10.1002/rcm.6703

Gershenzon, M., Davidovits, P., Jayne, J. T., Kolb, C. E., & Worsnop, D. R. (2001). Simultaneous uptake of DMS and ozone on water. *Journal of Physical Chemistry A*, *105*(29), 7031–7036. https://doi.org/10.1021/jp010696y

González-García, N., González-Lafont, A., & Lluch, J. M. (2007). Methanesulfinic acid reaction with OH: Mechanism, rate constants, and atmospheric implications. *Journal of Physical Chemistry A*, *111*(32), 7825–7832. https://doi.org/10.1021/jp0722455

Goto-Azuma, K., Hirabayashi, M., Motoyama, H., Miyake, T., Kuramoto, T., Uemura, R., et al. (2019). Reduced marine phytoplankton sulphur emissions in the Southern Ocean during the past seven glacials. *Nature Communications*, *10*(1). https://doi.org/10.1038/s41467-019-11128-6

Grannas, A. M., Jones, A. E., Dibb, J., Ammann, M., Anastasio, C., Beine, H. J., et al. (2007). An overview of snow photochemistry: Evidence, mechanisms and impacts. *Atmospheric Chemistry and Physics*, *7*(16), 4329–4373. https://doi.org/10.5194/acp-7-4329-2007

Grilli, R., Legrand, M., Kukui, A., Méjean, G., Preunkert, S., & Romanini, D. (2013). First investigations of IO, BrO, and $NO_2$ summer atmospheric levels at a coastal East Antarctic site using mode-locked cavity enhanced absorption spectroscopy. *Geophysical Research Letters*, *40*, 791–796. https://doi.org/10.1002/grl.50154

Hill-Falkenthal, J., Priyadarshi, A., Savarino, J., & Thiemens, M. (2013). Seasonal variations in $^{35}S$ and $\Delta^{17}O$ of sulfate aerosols on the Antarctic plateau. *Journal of Geophysical Research: Atmospheres*, *118*, 9444–9455. https://doi.org/10.1002/jgrd.50716

Hoffmann, E. H., Tilgner, A., Schrödner, R., Bräuer, P., Wolke, R., & Herrmann, H. (2016). An advanced modeling study on the impacts and atmospheric implications of multiphase dimethyl sulfide chemistry. *Proceedings of the National Academy of Sciences of the United States of America*, *113*(42), 11776–11781. https://doi.org/10.1073/pnas.1606320113

Holland, H. D., Lazar, B., & McCaffrey, M. (1986). Evolution of the atmosphere and oceans. *Nature*, *320*(6057), 27–33. https://doi.org/10.1038/320027a0

Holt, B. D., Kumar, R., & Cunningham, P. T. (1981). Oxygen-18 study of the aqueous-phase oxidation of sulfur dioxide. *Atmospheric Environment*, *15*(4), 557–566. https://doi.org/10.1016/0004-6981(81)90186-4

Huang, J., & Jaeglé, L. (2017). Wintertime enhancements of sea salt aerosol in polar regions consistent with a sea ice source from blowing snow. *Atmospheric Chemistry and Physics*, *17*(5), 3699–3712. https://doi.org/10.5194/acp-17-3699-2017

Huang, J., Jaeglé, L., Chen, Q., Alexander, B., Sherwen, T., Evans, M. J., et al. (2020). Evaluating the impact of blowing-snow sea salt aerosol on springtime BrO and $O_3$ in the Arctic. *Atmospheric Chemistry and Physics*, *20*(12), 7335–7358. https://doi.org/10.5194/acp-20-7335-2020

Huang, J., Jaeglé, L., & Shah, V. (2018). Using CALIOP to constrain blowing snow emissions of sea salt aerosols over Arctic and Antarctic sea ice. *Atmospheric Chemistry and Physics*, *18*(22), 16253–16269. https://doi.org/10.5194/acp-18-16253-2018

Ingham, T., Bauer, D., Sander, R., Crutzen, P. J., & Crowley, J. N. (1999). Kinetics and products of the reactions BrO + DMS and Br + DMS at 298 K. *Journal of Physical Chemistry A*, *103*(36), 7199–7209. https://doi.org/10.1021/jp9905979

Ishino, S., Hattori, S., Savarino, J., Jourdain, B., Preunkert, S., Legrand, M., et al. (2017). Seasonal variations of triple oxygen isotopic compositions of atmospheric sulfate, nitrate, and ozone at Dumont d'Urville, coastal Antarctica. *Atmospheric Chemistry and Physics*, *17*(5), 3713–3727. https://doi.org/10.5194/acp-17-3713-2017

Ishino, S., Hattori, S., Savarino, J., Legrand, M., Albalat, E., Albarede, F., et al. (2019). Homogeneous sulfur isotope signature in East Antarctica and implication for sulfur source shifts through the last glacial–interglacial cycle. *Scientific Reports*, *9*(1), 12378. https://doi.org/10.1038/s41598-019-48801-1

Jaeglé, L., Quinn, P. K., Bates, T. S., Alexander, B., & Lin, J.-T. (2011). Global distribution of sea salt aerosols: New constraints from in situ and remote sensing observations. *Atmospheric Chemistry and Physics*, *11*(7), 3137–3157. https://doi.org/10.5194/acp-11-3137-2011

Janssen, C., Guenther, J., Krankowsky, D., & Mauersberger, K. (2003). Temperature dependence of ozone rate coefficients and isotopologue fractionation in $^{16}O$–$^{18}O$ oxygen mixtures. *Chemical Physics Letters*, *367*(1–2), 34–38. https://doi.org/10.1016/S0009-2614(02)01665-2

Janssen, C., & Tuzson, B. (2006). A diode laser spectrometer for symmetry selective detection of ozone isotopomers. *Applied Physics B: Lasers and Optics*, *82*(3), 487–494. https://doi.org/10.1007/s00340-005-2044-6

Jeffery, C. A., & Austin, P. H. (1997). Homogeneous nucleation of supercooled water: Results from a new equation of state. *Journal of Geophysical Research*, *102*(21), 25269–25279. https://doi.org/10.1029/97JD02243

Johnston, J. C., & Thiemens, M. H. (1997). The isotopic composition of tropospheric ozone in three environments. *Journal of Geophysical Research*, *102*(21), 25395–25404. https://doi.org/10.1029/97JD02075

Jourdain, B., & Legrand, M. (2002). Year-round records of bulk and size-segregated aerosol composition and HCl and $HNO_3$ levels in the Dumont d'Urville (coastal Antarctica) atmosphere: Implications for sea-salt aerosol fractionation in the winter and summer. *Journal of Geophysical Research*, *107*(22), 4645. https://doi.org/10.1029/2002JD002471

Krankowsky, D., Bartecki, F., Klees, G. G., Mauersberger, K., Schellenbach, K., & Stehr, J. (1995). Measurement of heavy isotope enrichment in tropospheric ozone. *Geophysical Research Letters*, *22*(13), 1713–1716. https://doi.org/10.1029/95GL01436

Kukui, A., Bossoutrot, V., Laverdet, G., & Le Bras, G. (2000). Mechanism of the reaction of $CH_3SO$ with $NO_2$ in relation to atmospheric oxidation of dimethyl sulfide: Experimental and theoretical study. *Journal of Physical Chemistry A*, *104*(5), 935–946. https://doi.org/10.1021/jp993158i

Kunasek, S. A., Alexander, B., Steig, E. J., Sofen, E. D., Jackson, T. L., Thiemens, M. H., et al. (2010). Sulfate sources and oxidation chemistry over the past 230 years from sulfur and oxygen isotopes of sulfate in a West Antarctic ice core. *Journal of Geophysical Research*, *115*, D18313. https://doi.org/10.1029/2010JD013846

Lana, A., Bell, T. G., Simó, R., Vallina, S. M., Ballabrera-Poy, J., Kettle, A. J., et al. (2011). An updated climatology of surface dimethlysulfide concentrations and emission fluxes in the global ocean. *Global Biogeochemical Cycles*, *25*, GB1004. https://doi.org/10.1029/2010GB003850

Legrand, M., & Mayewski, P. (1997). Glaciochemistry of polar ice cores: A review. *Reviews of Geophysics*, *35*(3), 219–243. https://doi.org/10.1029/96RG03527

Legrand, M., Preunkert, S., Savarino, J., Frey, M. M., Kukui, A., Helmig, D., et al. (2016). Inter-annual variability of surface ozone at coastal (Dumont d'Urville, 2004–2014) and inland (Concordia, 2007–2014) sites in East Antarctica. *Atmospheric Chemistry and Physics*, *16*(12), 8053–8069. https://doi.org/10.5194/acp-16-8053-2016

Legrand, M., Preunkert, S., Weller, R., Zipf, L., Elsässer, C., Merchel, S., et al. (2017). Year-round record of bulk and size-segregated aerosol composition in central Antarctica (Concordia site)–Part 2: Biogenic sulfur (sulfate and methanesulfonate) aerosol. *Atmospheric Chemistry and Physics*, *17*(22), 14055–14073. https://doi.org/10.5194/acp-17-14055-2017

Legrand, M., Preunkert, S., Wolff, E., Weller, R., Jourdain, B., & Wagenbach, D. (2017). Year-round records of bulk and size-segregated aerosol composition in central Antarctica (Concordia site)—Part 1: Fractionation of sea-salt particles. *Atmospheric Chemistry and Physics*, *17*(22), 14039–14054. https://doi.org/10.5194/acp-17-14039-2017

Legrand, M., Yang, X., Preunkert, S., & Theys, N. (2016). Year-round records of sea salt, gaseous, and particulate inorganic bromine in the atmospheric boundary layer at coastal (Dumont d'Urville) and central (Concordia) East Antarctic sites. *Journal of Geophysical Research: Atmospheres*, *121*, 997–1023. https://doi.org/10.1002/2015JD024066

Legrand, M. R., Delmas, R. J., & Charlson, R. J. (1988). Climate forcing implications from Vostok ice-core sulphate data. *Nature*, *334*(6181), 418–420. https://doi.org/10.1038/334418a0

Listowski, C., Delanoë, J., Kirchgaessner, A., Lachlan-Cope, T., & King, J. (2019). Antarctic clouds, supercooled liquid water and mixed phase, investigated with DARDAR: Geographical and seasonal variations. *Atmospheric Chemistry and Physics*, *19*(10), 6771–6808. https://doi.org/10.5194/acp-19-6771-2019

Liu, Q., Schurter, L. M., Muller, C. E., Aloisio, S., Francisco, J. S., & Margerum, D. W. (2001). Kinetics and mechanisms of aqueous ozone reactions with bromide, sulfite, hydrogen sulfite, iodide, and nitrite ions. *Inorganic Chemistry*, *40*(17), 4436–4442. https://doi.org/10.1021/ic000919j

Liu, T., & Abbatt, J. P. D. (2020). An experimental assessment of the importance of S(IV) oxidation by hypohalous acids in the marine atmosphere. *Geophysical Research Letters*, *47*, e2019GL086465. https://doi.org/10.1029/2019GL086465

Lyons, J. R. (2001). Transfer of mass-independent fractionation in ozone to other oxygen-containing radicals in the atmosphere. *Geophysical Research Letters*, *28*(17), 3231–3234. https://doi.org/10.1029/2000GL012791

Matsuhisa, Y., Goldsmith, J. R., & Clayton, R. N. (1979). Oxygen isotopic fractionation in the system quartz–albite–anorthite–water. *Geochimica et Cosmochimica Acta*, *43*(7), 1131–1140. https://doi.org/10.1016/0016-7037(79)90099-1

Mauersberger, K., Krankowsky, D., & Janssen, C. (2003). *Oxygen isotope processes and transfer reactions* (pp. 265–279). Dordrecht, the Netherlands: Springer. https://doi.org/10.1007/978-94-010-0145-8_17

Mauldin, R. L., Eisele, F. L., Tanner, D. J., Kosciuch, E., Shetter, R., Lefer, B., et al. (2001). Measurements of OH, $H_2SO_4$ and MSA at the South Pole during ISCAT. *Geophysical Research Letters*, *28*(19), 3629–3632. https://doi.org/10.1029/2000GL012711

Minikin, A., Legrand, M., Hall, J., Wagenbach, D., Kleefeld, C., Wolff, E., et al. (1998). Sulfur-containing species (sulfate and methanesulfonate) in coastal Antarctic aerosol and precipitation. *Journal of Geophysical Research*, *103*(3339), 10975–10990. https://doi.org/10.1029/98JD00249

Morin, S., Savarino, J., Bekki, S., Gong, S., & Bottenheim, J. W. (2007). Signature of Arctic surface ozone depletion events in the isotope anomaly ($\Delta^{17}O$) of atmospheric nitrate. *Atmospheric Chemistry and Physics*, *7*(5), 1451–1469. https://doi.org/10.5194/acp-7-1451-2007

Morton, J., Barnes, J., Schueler, B., & Mauersberger, K. (1990). Laboratory studies of heavy ozone. *Journal of Geophysical Research*, *95*(D1), 901–907. https://doi.org/10.1029/JD095iD01p00901

Mungall, E. L., Wong, J. P. S., & Abbatt, J. P. D. (2018). Heterogeneous oxidation of particulate methanesulfonic acid by the hydroxyl radical: Kinetics and atmospheric implications. *ACS Earth and Space Chemistry*, *2*(1), 48–55. https://doi.org/10.1021/acsearthspacechem.7b00114

Murray, L. T., Mickley, L. J., Kaplan, J. O., Sofen, E. D., Pfeiffer, M., & Alexander, B. (2014). Factors controlling variability in the oxidative capacity of the troposphere since the Last Glacial Maximum. *Atmospheric Chemistry and Physics*, *14*(7), 3589–3622. https://doi.org/10.5194/acp-14-3589-2014

Noro, K., Hattori, S., Uemura, R., Fukui, K., Hirabayashi, M., Kawamura, K., et al. (2018). Spatial variation of isotopic compositions of snowpack nitrate related to post-depositional processes in eastern Dronning Maud Land, East Antarctica. *Geochemical Journal*, *52*(2), e7–e14. https://doi.org/10.2343/geochemj.2.0519

Park, R. J., Jacob, D. J., Field, B. D., & Yantosca, R. M. (2004). Natural and transboundary pollution influences on sulfate-nitrate-ammonium aerosols in the United States: Implications for policy. *Journal of Geophysical Research*, *109*, D15204. https://doi.org/10.1029/2003JD004473

Parrella, J. P., Jacob, D. J., Liang, Q., Zhang, Y., Mickley, L. J., Miller, B., et al. (2012). Tropospheric bromine chemistry: Implications for present and pre-industrial ozone and mercury. *Atmospheric Chemistry and Physics*, *12*(15), 6723–6740. https://doi.org/10.5194/acp-12-6723-2012

Patris, N., Delmas, R. J., & Jouzel, J. (2000). Isotopic signatures of sulfur in shallow Antarctic ice cores. *Journal of Geophysical Research*, *105*(D6), 7071–7078. https://doi.org/10.1029/1999JD900974

Pound, R. J., Sherwen, T., Helmig, D., Carpenter, L. J., & Evans, M. J. (2020). Influences of oceanic ozone deposition on tropospheric photochemistry. *Atmospheric Chemistry and Physics*, *20*(7), 4227–4239. https://doi.org/10.5194/acp-20-4227-2020

Preunkert, S., Jourdain, B., Legrand, M., Udisti, R., Becagli, S., & Cerri, O. (2008). Seasonality of sulfur species (dimethyl sulfide, sulfate, and methanesulfonate) in Antarctica: Inland versus coastal regions. *Journal of Geophysical Research*, *113*, D15302. https://doi.org/10.1029/2008JD009937

Preunkert, S., Legrand, M., Jourdin, B., Moulin, C., Belviso, S., Kasamatsu, N., et al. (2007). Interannual variability of dimethylsulfide in air and seawater and its atmospheric oxidation by-products (methanesulfonate and sulfate) at Dumont d'Urville, coastal Antarctica (1999–2003). *Journal of Geophysical Research*, *112*, D06306. https://doi.org/10.1029/2006JD007585

Pruett, L. E., Kreutz, K. J., Wadleigh, M., & Aizen, V. (2004). Assessment of sulfate sources in high-elevation Asian precipitation using stable sulfur isotopes. *Environmental Science and Technology*, *38*(18), 4728–4733. https://doi.org/10.1021/es035156o

Pruppacher, H. R. (1995). A new look at homogeneous ice nucleation in supercooled water drops. *Journal of the Atmospheric Sciences*, *52*(11), 1924–1933. https://doi.org/10.1175/1520-0469(1995)052<1924:ANLAHI>2.0.CO;2

Saiz-Lopez, A., Mahajan, A. S., Salmon, R. A., Bauguitte, S. J. B., Jones, A. E., Roscoe, H. K., & Plane, J. M. C. (2007). Boundary layer halogens in coastal Antarctica. *Science*, *317*(5836), 348–351. https://doi.org/10.1126/science.1141408

Savarino, J., Alexander, B., Darmohusodo, V., & Thiemens, M. H. (2001). Sulfur and oxygen isotope analysis of sulfate at micromole levels using a pyrolysis technique in a continuous flow system. *Analytical Chemistry*, *73*(18), 4457–4462. https://doi.org/10.1021/ac010017f

Savarino, J., Kaiser, J., Morin, S., Sigman, D. M., & Thiemens, M. H. (2007). Nitrogen and oxygen isotopic constraints on the origin of atmospheric nitrate in coastal Antarctica. *Atmospheric Chemistry and Physics*, *7*(8), 1925–1945. https://doi.org/10.5194/acp-7-1925-2007

Savarino, J., Lee, C. C. W., & Thiemens, M. H. (2000). Laboratory oxygen isotopic study of sulfur (IV) oxidation: Origin of the mass-independent oxygen isotopic anomaly in atmospheric sulfates and sulfate mineral deposits on Earth. *Journal of Geophysical Research*, *105*(D23), 29079–29088. https://doi.org/10.1029/2000JD900456

Savarino, J., & Thiemens, M. H. (1999). Analytical procedure to determine both $\delta^{18}O$ and $\delta^{17}O$ of $H_2O_2$ in natural water and first measurements. *Atmospheric Environment*, *33*(22), 3683–3690. https://doi.org/10.1016/S1352-2310(99)00122-3

Savarino, J., Vicars, W. C., Legrand, M., Preunkert, S., Jourdain, B., Frey, M. M., et al. (2016). Oxygen isotope mass balance of atmospheric nitrate at Dome C, East Antarctica, during the OPALE campaign. *Atmospheric Chemistry and Physics*, *16*(4), 2659–2673. https://doi.org/10.5194/acp-16-2659-2016

Schauer, A. J., Kunasek, S. A., Sofen, E. D., Erbland, J., Savarino, J., Johnson, B. W., et al. (2012). Oxygen isotope exchange with quartz during pyrolysis of silver sulfate and silver nitrate. *Rapid Communications in Mass Spectrometry*, *26*(18), 2151–2157. https://doi.org/10.1002/rcm.6332

Schmidt, J. A., Jacob, D. J., Horowitz, H. M., Hu, L., Sherwen, T., Evans, M. J., et al. (2016). Modeling the observed tropospheric BrO background: Importance of multiphase chemistry and implications for ozone, OH, and mercury. *Journal of Geophysical Research: Atmospheres*, *121*, 11819–11835. https://doi.org/10.1002/2015JD024229

Seinfeld, J. H., & Pandis, S. N. (2006). Chemistry of the Atmospheric Aqueous Phase. In J. H. Seinfeld & S. N. Pandis (Eds.), *Atmospheric chemistry and physics: From air pollution to climate change* (pp. 284–349). New York, USA: Wiley & Sons.

Sherwen, T., Evans, M. J., Carpenter, L. J., Andrews, S. J., Lidster, R. T., Dix, B., et al. (2016). Iodine's impact on tropospheric oxidants: A global model study in GEOS-Chem. *Atmospheric Chemistry and Physics*, *16*(2), 1161–1186. https://doi.org/10.5194/acp-16-1161-2016

Sherwen, T., Schmidt, J. A., Evans, M. J., Carpenter, L. J., Großmann, K., Eastham, S. D., et al. (2016). Global impacts of tropospheric halogens (Cl, Br, I) on oxidants and composition in GEOS-Chem. *Atmospheric Chemistry and Physics*, *16*(18), 12239–12271. https://doi.org/10.5194/acp-16-12239-2016

Simpson, W. R., Von Glasow, R., Riedel, K., Anderson, P., Ariya, P., Bottenheim, J., et al. (2007). Halogens and their role in polar boundary-layer ozone depletion. *Atmospheric Chemistry and Physics*, *7*(16), 4375–4418. https://doi.org/10.5194/acp-7-4375-2007

Sofen, E. D., Alexander, B., Steig, E. J., Thiemens, M. H., Kunasek, S. A., Amos, H. M., et al. (2014). WAIS divide ice core suggests sustained changes in the atmospheric formation pathways of sulfate and nitrate since the 19th century in the extratropical Southern Hemisphere. *Atmospheric Chemistry and Physics*, *14*(11), 5749–5769. https://doi.org/10.5194/acp-14-5749-2014

Tian, Y., Tian, Z. M., Wei, W. M., He, T. J., Chen, D. M., & Liu, F. C. (2007). Ab initio study of the reaction of OH radical with methyl sulfinic acid (MSIA). *Chemical Physics*, *335*(2–3), 133–140. https://doi.org/10.1016/j.chemphys.2007.04.009

Theys, N., Van Roozendael, M., Hendrick, F., Yang, X., De Smedt, I., Richter, A., et al. (2011). Global observations of tropospheric BrO columns using GOME-2 satellite data. *Atmospheric Chemistry and Physics*, *11*(4), 1791–1811. https://doi.org/10.5194/acp-11-1791-2011

Thiemens, M. H., & Jackson, T. (1990). Pressure dependency for heavy isotope enhancement in ozone formation. *Geophysical Research Letters*, *17*(6), 717–719. https://doi.org/10.1029/GL017i006p00717

Troy, R. C., & Margerum, D. W. (1991). Non-metal redox kinetics: Hypobromite and hypobromous acid reactions with iodide and with sulfite and the hydrolysis of bromosulfate. *Inorganic Chemistry*, *30*(18), 3538–3543. https://doi.org/10.1021/ic00018a028

Vicars, W. C., & Savarino, J. (2014). Quantitative constraints on the $^{17}$O-excess ($\Delta^{17}$O) signature of surface ozone: Ambient measurements from 50°N to 50°S using the nitrite-coated filter technique. *Geochimica et Cosmochimica Acta*, *135*, 270–287. https://doi.org/10.1016/j.gca.2014.03.023

von Glasow, R., & Crutzen, P. J. (2004). Model study of multiphase DMS oxidation with a focus on halogens. *Atmospheric Chemistry and Physics*, *4*(3), 589–608. https://doi.org/10.5194/acp-4-589-2004

Wagenbach, D., Ducroz, F., Mulvaney, R., Keck, L., Minikin, A., Legrand, M., et al. (1998). Sea-salt aerosol in coastal Antarctic regions. *Journal of Geophysical Research*, *103*(3339), 10961–10974. https://doi.org/10.1029/97JD01804

Wagnon, P., Delmas, R. J., & Legrand, M. (1999). Loss of volatile acid species from upper firn layers at Vostok, Antarctica. *Journal of Geophysical Research*, *104*(D3), 3423–3431. https://doi.org/10.1029/98JD02855

Walters, W. W., Michalski, G., Böhlke, J. K., Alexander, B., Savarino, J., & Thiemens, M. H. (2019). Assessing the seasonal dynamics of nitrate and sulfate aerosols at the South Pole utilizing stable isotopes. *Journal of Geophysical Research: Atmospheres*, *124*, 8161–8177. https://doi.org/10.1029/2019JD030517

Wang, L., & Zhang, J. (2002). Ab initio study of reaction of dimethyl sulfoxide (DMSO) with OH radical. *Chemical Physics Letters*, *356*(5–6), 490–496. https://doi.org/10.1016/S0009-2614(02)00397-4

Weller, R., Traufetter, F., Fischer, H., Oerter, H., Piel, C., & Miller, H. (2004). Postdepositional losses of methane sulfonate, nitrate, and chloride at the European Project for Ice Coring in Antarctica deep-drilling site in Dronning Maud Land, Antarctica. *Journal of Geophysical Research*, *109*, D07301. https://doi.org/10.1029/2003JD004189

Wolff, E. W., Fischer, H., Fundel, F., Ruth, U., Twarloh, B., Littot, G. C., et al. (2006). Southern Ocean sea-ice extent, productivity and iron flux over the past eight glacial cycles. *Nature*, *440*(7083), 491–496. https://doi.org/10.1038/nature04614

Zatko, M., Geng, L., Alexander, B., Sofen, E., & Klein, K. (2016). The impact of snow nitrate photolysis on boundary layer chemistry and the recycling and redistribution of reactive nitrogen across Antarctica and Greenland in a global chemical transport model. *Atmospheric Chemistry and Physics*, *16*(5), 2819–2842. https://doi.org/10.5194/acp-16-2819-2016

Zhang, J., Miau, T.-T., & Lee, Y. T. (1997). Crossed molecular beam study of the reaction Br + $O_3$. *Journal of Physical Chemistry A*, *101*(37), 6922–6930. https://doi.org/10.1021/jp970860a

Zhu, L. (2004). *Aqueous phase reaction kinetics of organic sulfur compounds of atmospheric interest* (dissertation). Atlanta, GA: Georgia Institute of Technology. Retrieved from http://hdl.handle.net/1853/4870

Zhu, L., Nicovich, J. M., & Wine, P. H. (2003a). Temperature-dependent kinetics studies of aqueous phase reactions of hydroxyl radicals with dimethylsulfoxide, dimethylsulfone, and methanesulfonate. *Aquatic Sciences*, *65*(4), 425–435. https://doi.org/10.1007/s00027-003-0673-6

Zhu, L., Nicovich, J. M., & Wine, P. H. (2003b). Temperature-dependent kinetics studies of aqueous phase reactions of $SO_4^-$ radicals with dimethylsulfoxide, dimethylsulfone, and methanesulfonate. *Journal of Photochemistry and Photobiology A: Chemistry*, *157*(2–3), 311–319. https://doi.org/10.1016/S1010-6030(03)00064-9